

Distinctive Phytoplankton Size Responses to the Nutrient Enrichment of Coastal Upwelling and Winter Convection in the Eastern Arabian Sea

^{1,2} Albin, K.J., *¹Jyothibabu, R., ¹Alok, K.T., ¹Santhikrishnan, S., ¹Sarath, S.,
³Sudheesh, V., ³Sherin, C.K., ¹Balachandran, K.K., ³Asha Devi, C.R., ³Gupta, G.V.M

¹CSIR - National Institute of Oceanography, Regional Centre, Kochi, INDIA

² Research Student, Bharathidasan University, Tiruchirappalli, INDIA

³Centre for Marine Living Resources and Ecology, Ministry of Earth Sciences, Kochi, INDIA

* Corresponding author: rjyothibabu@nio.org

Abstract

Even though the seasonal pattern of phytoplankton biomass distribution in the seas around India is reasonably well understood, there is relatively little information on phytoplankton size classes. The current study shows how phytoplankton of different size classes respond to nutrient enrichment caused by vertical convective mixing during the Northeast Monsoon [(NEM) November-February] and coastal upwelling during the Southwest Monsoon [(SWM) June-September] in the Eastern Arabian Sea (EAS). In the Northeastern Arabian Sea (NEAS), phytoplankton biomass [Chlorophyll-a (Chl-a)] and primary production (PP) were moderate and comparable during both the NEM (Chl-a av. 21 mg m⁻² and PP av. 601 mg C m⁻² d⁻¹) and the SWM (Chl-a av. 27 mg m⁻² and PP av. 516 mg C m⁻² d⁻¹). The Southeastern Arabian Sea (SEAS) was oligotrophic (Chl-a av. 12 mg m⁻² and PP av. 197 mg C m⁻² d⁻¹) during the NEM due to strong surface stratification, but due to coastal upwelling, it turned into a very productive system along the shelf waters during the SWM (Chl-a av. 45 mg m⁻² and PP av. 1201 mg C m⁻² d⁻¹). Interestingly, the subsurface Chl-a maximum (SCM) was almost absent in the NEAS during both seasons. Similarly, SCM was absent in the entire coastal upwelling zone of the EAS during the SWM. In these areas and situations, Chl-a was found to accumulate in the nutrient-rich surface layers of the shallow euphotic zones. The nutrient enrichment of the coastal upwelling along the shelf waters in the EAS favoured the growth of larger micro-and meso-phytoplankton during the SWM [av. 43.8 mg m⁻² (av. 65.9% total Chl-a)], whereas the entire NEAS favoured the growth of nano-phytoplankton during the NEM [av. 13.9 mg m⁻² (av. 64.8% total Chl-a)]. Differences in the physical processes enabling the entrainment of nutrients (Nitrate (NO₃), Phosphate (PO₄) and silicate (SiO₄)] into the euphotic layer could explain the observed differences in the phytoplankton size fractions. The convective mixing in the NEAS during the NEM erodes the bottom of the mixed layer (50-120 m), resulting in only moderate enrichment of NO₃ (av. 0.62 ± 0.45 μM) and SiO₄ (av. 3.01 ± 0.83 μM), and low level of PO₄ (av. 0.49 ± 0.13 μM) in the mixed layer (av. 60 m). This caused N -limitation in the NEAS, which favoured the dominance of nano-phytoplankton. Alternatively, coastal upwelling during the SWM drives deeper subsurface waters (75-150 m) into the shallow surface mixed layer (av. 30 m) in shelf water, causing significant enrichment of NO₃ (av. 11.02 ± 3.55 μM), SiO₄ (av. 18.34 ± 11.37 μM) and PO₄ (av. 1.15 ± 0.21 μM). The enhanced nutrients in the coastal upwelling zones favoured the dominance of larger micro and meso-phytoplankton. However, during the SWM, the oceanic waters of the entire EAS showed low nutrient concentration compared to the shelf waters, which favoured the dominance of nanophytoplankton. In conclusion, our work reveals the large contribution of nano-phytoplankton in Chl-a biomass across the entire EAS, underlining their ecological relevance in both N-limited and N-enriched environments.

Keywords: Phytoplankton, upwelling, convective mixing, nutrient enrichment, Arabian Sea

1. Introduction

India produced 37.27 lakh tonnes of marine fish in the fiscal year 2019-2020, with its west coast accounting for 21.75 lakh tonnes (~60 %) (Department of Fisheries, 2020). This signifies the vast marine fishing resources available along the west coast of India in the eastern Arabian Sea, and so better knowledge of its environmental features and its linkages to plankton quality and quantity has great scientific relevance (Madhupratap et al., 2001; Jyothibabu et al., 2010; George et al., 2012; Shankar et al., 2019). Phytoplankton, which is found at the base of the marine food web, are consumed by all other aquatic species, including fish (Cushing, 1989; Mann, 1993; Pomeroy, 2000). Studies have revealed remarkable synchrony between phytoplankton and the peak production of fish larvae, which is critical for larval survival and later recruitment into fish stocks (Sherman et al., 1984; Binu, 2003; Platt et al., 2003; George et al., 2012; Menon et al., 2019). Studies showed that the food web along India's southwest coast is more suited for herbivorous fishes (sardine and mackerel), whereas the food web along India's northwest coast favours carnivorous fishes (Bombay duck, croakers, and ribbon fishes) (Chidambaram, 1945; Madhupratap et al., 2001; Shankar et al., 2019).

Phytoplankton of different size classes [pico (0.2 - 2 μm), nano (2 - 20 μm), micro (20 - 200 μm) and meso (>200 μm)] are unevenly distributed in the ocean mainly due to their varying nutrient requirements (bottom-up control) and grazing pressure (top-down control) (Malone 1980; Banse et al., 1996; Madhu et al., 2010; Karnan et al., 2017a; Jyothibabu et al., 2018a, b). In the tropics, studies, in general, show the key role of nutrients in structuring the phytoplankton size classes (Banse and McClain., 1986; Garrison et al., 1998; Karnan et al., 2017a, b; Burson et al., 2018; Jiang et al., 2019), while little is known about any top-down control (Banse et al., 1996). At large, nutrient-rich environments favour larger phytoplankton (centric and chain-forming diatoms, dinoflagellates), whereas the nutrient-depleted (oligotrophic) environments facilitate the dominance of smaller diatoms, phytoflagellates, and cyanobacteria (Chisholm 1992; Guenther et al., 2015; Karnan et al., 2017a; Jyothibabu et al., 2018a). As a consequence, larger phytoplankton cause the dominance of an efficient and short (classical) food chain, while smaller phytoplankton leads to the development of a less efficient and long (microbial) food web (Pomeroy 1974; Azam et al., 1983; Landry et al., 2002; Irwin et al., 2006). The existence of an efficient short food chain is considered to be the primary reason for the nutrient-rich upwelling systems that occupy only 0.1% of the total ocean area and contribute to 20% of the world's fish production (Mann, 1993; Cury et al., 2000). Even though many studies on the seasonal oceanographic setting in the EAS are available, many aspects regarding how distinctly ocean processes govern the growth of different phytoplankton size classes are still unclear. This aspect is

very crucial to know the bottom-up control of fishery resources (Cushing, 1989; Mann, 1993; Pomeroy, 2000; Madhupratap et al., 2001).

The Arabian Sea, in general, is a productive basin compared to the Bay of Bengal, primarily due to the diverse processes such as upwelling during the SWM and convective mixing during the NEM (Jyothibabu et al., 2010; 2021). In the Arabian Sea itself, the phytoplankton biomass in the western Arabian Sea is much higher than in the EAS due to the entrainment of more nutrients into the euphotic column (Banse and McClain, 1986; Levy et al., 2007; Jyothibabu et al., 2010). Even in the EAS, the NEAS has noticeably higher phytoplankton biomass compared to the SEAS. The high phytoplankton biomass in the NEAS is sustained for almost 9 months [June to September of the SWM, November to February of the NEM, and March-April of the Spring Intermonsoon (SIM)], compared to 4 months [SWM (June to September)] in the SEAS (Jyothibabu et al., 2010; Shankar et al., 2019). Therefore, the SEAS experiences an oligotrophic condition during the Spring Intermonsoon (SIM) and the NEM due to strong surface layer stratification arising from the combined effect of relatively high solar heating and the intrusion of low saline Bay of Bengal waters (Jyothibabu et al., 2008; 2010; Asha Devi et al., 2010). Unlike the NEAS, the SEAS has a well-marked seasonality in nutrients and phytoplankton biomass with a significantly high during the SWM and a low during the rest of the year (Jyothibabu et al., 2008; 2010).

Earlier studies of phytoplankton in the EAS had low sample resolution (Bhattathiri et al., 1996; Habeebrehman et al., 2008) or extremely limited spatial coverage (Madhu et al., 2010, 2017; Karnan et al., 2017a, b), with some focusing primarily on a specific component such as picoplankton (Roy and Anil., 2015; Bernal et al., 2018, 2019; Vijayan et al., 2021), resulting in the absence of integrated data. Some researchers used empirical relationships to describe the qualitative characteristics of phytoplankton marker pigments (Ahamed et al., 2016; Rao et al., 2018; Vijayan et al., 2021). However, several of the important marker pigments for diatoms and dinoflagellates have contributions from nano-, micro-, and meso-phytoplankton sizes, so the approach based on marker pigments has limitations in quantifying phytoplankton size classes (Mackey et al., 1996; Karnan et al., 2017a; 2020). The major objectives of this study are to (a) quantify the contribution of different phytoplankton size classes to the total community biomass in the EAS during the upwelling (SWM) and convective mixing (NEM) periods, and (b) identify the factors/mechanisms responsible for the phytoplankton size class patterns in the EAS. This study combines traditional approaches with modern plankton quantification tools like FlowCAM, flow cytometry, and satellite remote sensing to achieve these objectives.

2. Materials and Methods

2.1. Study area and field sampling

The EAS, bordered by the western coastline of India, experiences seasonally reversing monsoon winds and ocean surface currents, both playing a major role in structuring the pattern of the phytoplankton community. The primary data for this study in the EAS (6°N to 23°N) was obtained from the research cruises during the NEM (January-February 2018) and the SWM (August 2018), the former onboard FORV *Sagar Sampada* and the latter onboard ORV *Sagar Kanya*. The sampling was carried out along six cross-shore transects (3 each in SEAS and NEAS) with several sampling points in each transect extending from the coastal (10 m) to oceanic (2000 m) regions (Figure 1). There were 36 locations from 6 cross-shore transects (T1 to T6). The southernmost transect was off Cape Comorin/Kanyakumari (T1 at 8°N) and the northernmost transect was off Okha (T6 at 22°N). The midway transects were Kochi (T2 at 10°N), Mangalore (T3 at 13°N), Mumbai (T4 at 19°N) and Veraval (T5 at 20°N). Locations in each transect were numbered serially based on bathymetry as stations 1, 2, 3, 4, 5, 6 and 7 to represent depths of 10, 20, 30, 50, 100, 1000 and 2000 m, respectively (Figure 1).

2.2. Data and Methods

The meteorological and oceanographic data used in the current study include the sea surface temperature [SST; [https://giovanni.gsfc.nasa.gov/\(MODIS Aqua\)](https://giovanni.gsfc.nasa.gov/(MODIS%20Aqua))], sea surface salinity (SSS) and surface wind [[https://oceanwatch.pifsc.noaa.gov/\(Miras SMOS and ASCAT respectively\)](https://oceanwatch.pifsc.noaa.gov/(Miras%20SMOS%20and%20ASCAT%20respectively))]. In addition, the ocean colour data for Chl-a during the years 2002-19 was used to synoptically represent the distribution of phytoplankton biomass in the SEAS and the NEAS [[https://oceancolor.gsfc.nasa.gov/\(MODIS Aqua\)](https://oceancolor.gsfc.nasa.gov/(MODIS%20Aqua))]. Satellite-derived euphotic depth based on Lee et al., (2007) was also used to understand its spatio-temporal variation [[https://oceanwatch.pifsc.noaa.gov/\(MODIS aqua\)](https://oceanwatch.pifsc.noaa.gov/(MODIS%20aqua))]. The satellite data sets were processed and visualised using Ferret v7.1, SeaDAS v7.5.3 and Ocean Data View v4.5.1. The vertical profiles of temperature, salinity, dissolved oxygen (DO) and Chl-a were obtained using a Conductivity Temperature Depth (CTD) profiler (Seabird electronics, USA) at each location. The mixed layer depth (MLD) at each station was determined from the CTD density data as the depth at which the density increases by 0.2 kg m⁻³ of the surface value.

Water samples for the analysis of various chemical and biological parameters were collected using 12 L Niskin bottles mounted on the CTD rosette frame. Water samples were collected from standard depths (0, 10, 20, 30, 50, 75, and 100 m) and used for measuring dissolved oxygen, macronutrients,

Chl-a, and PP. DO, macronutrients [nitrate (NO_3), phosphate (PO_4), and silicate (SiO_4)] were measured based on Grasshoff et al., (1999). Nitrite (NO_2) was analysed based on the method of Garcia-Robledo et al (2014) and all the macronutrients were measured using the SKALAR SAN++ Autoanalyzer (detection limit for $\text{NO}_3 \pm 0.027 \mu\text{M}$, $\text{NO}_2 \pm 0.005 \mu\text{M}$, $\text{PO}_4 \pm 0.009 \mu\text{M}$ and $\text{SiO}_4 \pm 0.037 \mu\text{M}$). The Chl-a data retrieved from the wet lab sensor-based CTD was corrected statistically using the data obtained from measuring Chl-a in the water samples at standard depths using a lab fluorometer (Jyothibabu et al., 2015, 2018b; Sarma et al., 2019). This is important as a recent study comparing the global Chl-a data retrieved from the CTD sensor and laboratory analysed (fluorometer) data showed that the former has a certain level of overestimation (Roesler et al., 2017). In the present study, we obtained a significant positive correlation between the CTD sensor and lab fluorometer datasets of Chl-a [NEM ($R^2 = 0.82$, $n = 198$, $y = 0.58 \times \text{CTD data} + 0.06$); SWM ($R^2 = 0.80$, $n = 201$, $y = 0.82 \times \text{CTD data} + 0.02$, $p < 0.0001$)]. The corrected values were used to develop the seasonal vertical distribution of Chl-a along the 6 cross-shore transects in the EAS.

The fluorometric analysis of Chl-a was carried out by filtration (1 to 2 L) of water samples on membrane filters (0.2 μm), depending up on the phytoplankton cells in the water, and subsequent extraction in 10 ml of 90% acetone. The extracted Chl-a was measured using a Turner design fluorometer (Trilogy, Turner Designs, USA; detection limit $0.025 \mu\text{g L}^{-1}$) (UNESCO, 1994). The quantification of phytoplankton size classes was based on a standard stepwise serial filtration of water samples (Jiao and Ni, 1997; Jyothibabu et al., 2015; 2018a; Sarma et al., 2016; Madhu et al., 2017; Brewin et al., 2019). In this study, the samples collected from all locations were separated on filters into different sizes, such as pico (0.2 - 3 μm), nano (3 - 20 μm), micro (20 - 200 μm), and meso (>200 μm) plankton. The phytoplankton size classes concentrated on different filter papers were then extracted in 10 ml of 90% acetone and measured fluorometrically following the standard procedure of Chl-a analysis (UNESCO, 1994). PP was estimated at selected locations in each transect (one location each in the coastal and oceanic waters) based on the ^{14}C assimilation method. A simulated in-situ incubation was followed by using a calibrated neutral density filter on light bottles during incubation to simulate the natural light intensity (UNESCO, 1994). The incubation experiment was carried out in a fibre tank equipped with an overflowing/running seawater facility, which was carried out for 6 hours (6 am to 12 pm) and the samples after the incubation were filtered through GF/F filters. The filters were stored in 7 ml scintillation vials, which were then exposed to 5 ml Cocktail-T for 24 hrs and then analysed on a liquid scintillation counter (TriCarb 2810TR, Perkin Elmer).

The composition of phytoplankton size classes was studied using a combination of Flow Cytometry and FlowCAM. Autotrophic pico- and nano- plankton samples were collected from PP locations, fixed with 1% glutaraldehyde in cryovials and stored at -80°C for enumeration using a BD Accuri C6 Flow Cytometer (Vaulot et al., 1996). Autotrophic prokaryotes (*Synechococcus*), picoeukaryotes and nanoplankton were quantified using scatter plots (flow cytogram) following Moreira-Turcq and Martin (1998) and Mohan et al., (2016). Prochlorophytes are not accounted for in this study (though measured) due to the low sensitivity of the BD Accuri C6 Flow Cytometer to them (Ribeiro et al., 2016). Microplankton composition and abundance were quantified using a FlowCAM VS4 following the standard method (Karnan et al., 2017a). Multiple correlations of Redundancy analysis (RDA) were used to understand the ecological linkage between physicochemical and biological variables of different seasons (Clarke and Warwick., 2001). RDA is a statistical direct gradient analysis technique used to extract and summarise the variation in a set of response variables that can be explained by a set of explanatory variables based on linear relationships between them.

3. Results

3.1. Physical variables

During the NEM, the northeasterly winds were moderate (av. $4.79 \pm 0.54 \text{ m s}^{-1}$) in the NEAS and weak (av. $3.88 \pm 0.32 \text{ m s}^{-1}$) in the SEAS. The atmosphere was cooler (av. $24.86 \pm 1.63^{\circ}\text{C}$) in the NEAS than in the SEAS (av. $26.32 \pm 0.82^{\circ}\text{C}$) (Table 1). As a consequence, SST was noticeably lower (av. $25.3 \pm 1.2^{\circ}\text{C}$) in the NEAS compared to the SEAS (av. $28.14 \pm 0.27^{\circ}\text{C}$) (Figure 2; Table 1). SSS was higher (av. 35.84 ± 0.36) in the NEAS compared to the SEAS (av. 33.21 ± 0.7). The overall mixed layer depth (MLD) was also high (av. $43.88 \pm 21.51 \text{ m}$) in the NEAS compared to the SEAS (av. $27.89 \pm 14.61 \text{ m}$). MLD variation during the NEM in the NEAS and the SEAS were noticeably lower in the inshore region (av. $33.75 \pm 13.83 \text{ m}$ and av. $25.33 \pm 12.12 \text{ m}$, respectively) as compared to the offshore region (av. 52.88 ± 23.75 and av. 30.44 ± 17.08 , respectively). The overall euphotic depth was found lower in the NEAS (av. $27.7 \pm 14.36 \text{ m}$) compared to the SEAS (av. $59.11 \pm 32.25 \text{ m}$), especially in the shelf waters (Figure 2; Table 1).

Winds were strong and southwesterly in the NEAS (av. $7.39 \pm 0.3 \text{ m s}^{-1}$) and northerly/northwesterly (av. $5.75 \pm 0.39 \text{ m s}^{-1}$) in the SEAS during the SWM. During this time, the air temperature varied minimally between the NEAS (av. $26.23 \pm 0.4^{\circ}\text{C}$) and the SEAS (av. $27.5 \pm 2.02^{\circ}\text{C}$). In the whole EAS, but especially in the SEAS, there was a general cooling trend closer to the Indian shoreline. In the NEAS, the SST followed the geographical trend of air temperature, cooling as it approached the shelf zone (Figure 2; Table 1). During the SWM, SST in the SEAS was considerably warmer offshore

than coastal, resulting in a distinct coastal-offshore gradient. During the SWM, SSS (av. 35.86 ± 0.74) was high throughout the EAS, with saltier waters (av. 36.39 ± 0.82) in the NEAS. During the SWM, MLD was markedly shallow (av. 10.5 ± 6.4 m) all along the coastal regions, contrasting to a deep MLD (av. 30.1 ± 15.2 m) offshore. The euphotic depth in the coastal section of the SEAS was also low (av. 16.3 ± 6.41 m) during the period, compared to the NEAS (av. 20.6 ± 8.11 m) (Figure 2; Table 1).

The thermohaline characteristics of the 6 cross-shore transects (T1 to T6) showed visible spatial and seasonal variations within and between the NEAS and the SEAS. During the NEM, the entire surface water column in the NEAS was cooler compared to the SEAS (Figures 3). The maximum cooling was found at T6 in the NEAS, which progressively decreased towards T5 and T3, more evidently in the shelf waters, whereas the SEAS was warmer and low saline (Figure 3). During the SWM, the offshore waters in the NEAS were warmer (>26 °C) than the coastal region (Figure 4). There were signatures of the upheaval of subsurface isotherms towards the coast in the NEAS, which was clearer along the northernmost transect (T6). Even though the entire EAS was high saline during the SWM, still there were lenses of low saline waters near the coastal region at T4, T3 and T2. Similar to the signature in the vertical temperature profiles in the NEAS during the SWM, the salinity profile also showed an upheaval trend towards the coast. Similar to the NEAS during the SWM, the surface (40 m) layer offshore of SEAS was also warmer compared to the coastal waters. A clear upheaval of subsurface isotherms towards the coast was well marked in all the cross-shore transects in the SEAS (T1 to T3). The overall salinity was high in the NEAS compared to the SEAS transects. In short, the SWM was characterised by the upheaval of subsurface waters over the entire western shelf sampled, but less prominently along with T4 (off Mumbai).

3.2. Chemical variables and their ratios

During the NEM, the upper euphotic column was generally saturated with DO (>150 μM). However, oxygen-deficient conditions (DO <100 μM) were always present in the subsurface waters, which was even traceable in shallow regions in the NEAS (T4 to T6; Figure 5). NO_3 in the upper euphotic column was moderately high (av. 4.13 μM) in the NEAS compared to the SEAS (av. 0.20 μM). PO_4 was low (<0.5 μM) in the offshore surface layers along all transects, though it was relatively high in the NEAS compared to the SEAS (Supplementary Figure 1). SiO_4 was present at moderate levels at all transects with an increasing gradient towards the north (Table 1). Overall, the nutrient concentrations in the upper 30 m were moderately high (av. NO_3 - 4.13 μM and av. SiO_4 - 6.53 μM) in the NEAS and significantly low in the SEAS (av. NO_3 - 0.20 μM and av. SiO_4 - 2.71 μM). The nutrient ratios varied noticeably over the spatial scale during the NEM. N/P ratio during the NEM was found

to be the highest in the coastal waters of the NEAS (av. 7.38 ± 4.42) followed by the offshore waters of the SEAS (av. 6.04 ± 1.91) (Table 1). N/Si ratio during the period showed a reverse trend with the highest in the offshore waters of the SEAS (av. 0.92 ± 0.29) followed by coastal waters of the NEAS (av. 0.77 ± 0.39). On the other hand, the Si/P ratio was the highest in the coastal waters of the SEAS (av. 10.6 ± 4.13) followed by the coastal waters of the NEAS (av. 9.63 ± 5.05).

During the SWM, the oxygen-deficient waters ($<50 \mu\text{M}$) that were situated below 100 m depth offshore during the NEM, get advected to the surface waters in the nearshore region (Figure 6). This shoaling up of the subsurface waters towards the coast sustained a high concentration of NO_3 in the nearshore waters over the entire EAS (Figure 6). A similar trend was evident in the case of PO_4 and SiO_4 (Supplementary Figure 2). Thus, an overall eutrophic condition was found in the EAS and, spatially, the enrichment of NO_3 and SiO_4 was markedly higher in the coastal region of the SEAS (av. $7.95 \mu\text{M}$ and av. $11.26 \mu\text{M}$, respectively) as compared to the NEAS (av. $3.78 \mu\text{M}$ and $4.57 \mu\text{M}$, respectively) (Table 1). The most striking of these high nutrient levels in the EAS is a ten-fold increase in NO_3 and a six-fold increase in SiO_4 in the coastal waters of the SEAS compared to the NEM period. But it is very relevant to note that the entire oceanic region of the EAS during the SWM had a noticeably lower concentration of all the nutrients compared to the shelf waters (Table 1). Overall, all the nutrient ratios of N and Si have noticeably increased in the SEAS during the SWM. N/P ratio during the SWM was found to be the highest in the coastal waters of the SEAS (av. 11.21 ± 2.6) followed by the offshore waters of the SEAS (av. 7.79 ± 3.52) (Table 1). The N/Si ratio during the period was the highest in the offshore waters of the SEAS (av. 1.57 ± 0.49) followed by the offshore waters of the NEAS (av. 1.43 ± 0.65). On the other hand, the Si/P ratio was the highest in the coastal waters of the SEAS (av. 16.52 ± 11.76) followed by the coastal waters of the NEAS (av. 7.82 ± 3.28).

3.3. Biological variables

3.3.1. Chl-a and PP

The synoptic satellite images of phytoplankton biomass (Chl-a) in the EAS during the NEM and the SWM are presented in Figure 7. Noticeable spatial variations in Chl-a were evident during both seasons. During the NEM, Chl-a was very low (av. $11.9 \pm 7.1 \text{ mg m}^{-2}$) in the shelf waters of the SEAS, whereas it was relatively high (av. $21.1 \pm 8.2 \text{ mg m}^{-2}$) in the NEAS. Conversely, during the SWM, the Chl-a was generally high over the entire EAS shelf with a substantial increase in the SEAS. The Chl-a profiles along the cross-shore transects showed wide spatiotemporal variations (Figure 8). During the NEM, there was no SCM in the NEAS, instead, a thick layer of high Chl-a ($> 0.8 \text{ mg m}^{-2}$) was found in the surface ($\sim 50 \text{ m}$) at T6 and T5, which progressively eroded to a feeble layer towards the

south (Figure 8). In the NEAS, Chl-a was low in the offshore region, which increased rapidly towards the coastal region. In the SEAS, however, there was a layer of SCM (Chl-a 0.3 mg m^{-3}) that gradually narrowed down towards the south (T1). The situation was different during the SWM with a thick surface layer of Chl-a along the entire coast up to 100 m depth zone from the coast and further offshore its concentration noticeably decreased towards 2000 m depth. Even in the oceanic 2000m depth zone, relatively high Chl-a concentration was found in the surface layers with an exception of an isolated subsurface maximum at 40-60 m depth at T1. Overall, the Chl-a during the NEM exhibited a surface layer maximum in the NEAS and a subsurface maximum in the SEAS, whereas the surface waters of the entire EAS was Chl-a rich during the SWM.

The integrated water column Chl-a (Figure 9, Table 1) showed enhanced phytoplankton biomass in the coastal waters [NEM (av. 22.7 mg m^{-2}) and the SWM (av. 82.2 mg m^{-2})] than in the offshore region [(NEM (av. 12.9 mg m^{-2}) and the SWM (av. 15.7 mg m^{-2})]. The satellite imagery also showed that Chl-a was moderately high in the NEAS during the NEM, while it remained significantly high over the entire EAS shelf during the SWM. The column Chl-a showed a notable increase in the inshore regions of SEAS (T1: 125.8 mg m^{-2} and T2: 101 mg m^{-2}) over the NEAS (T6: 72.1 mg m^{-2}). The spatiotemporal pattern of PP was very similar to Chl-a with two distinct seasonal peaks in the entire EAS (Table 1). The coastal water in the entire EAS has higher PP than the offshore waters regardless of seasons (Table 1). The NEAS had moderate PP during the NEM (av. $601 \pm 269 \text{ mgC m}^{-2} \text{ d}^{-1}$) and the SWM (av. $516 \pm 158 \text{ mgC m}^{-2} \text{ d}^{-1}$). On the other hand, the SEAS had an exceptionally high PP during the SWM (av. $1201 \pm 752 \text{ mgC m}^{-2} \text{ d}^{-1}$) and a noticeably low PP during the NEM (av. $196 \pm 49 \text{ mgC m}^{-2} \text{ d}^{-1}$). Unlike the SWM that had high PP in the coastal regions of the entire EAS [(SEAS av. $1571 \pm 666 \text{ mgC m}^{-2} \text{ d}^{-1}$); (NEAS av. $516.2 \pm 158 \text{ mgC m}^{-2} \text{ d}^{-1}$)], the NEM had relatively high PP only in the coastal waters of the NEAS (av. $784 \pm 106 \text{ mgC m}^{-2} \text{ d}^{-1}$) (Figure 9). But very evidently, the coastal water of the SEAS was significantly more productive during the SWM (av. $1571 \pm 666 \text{ mgC m}^{-2} \text{ d}^{-1}$) as compared to the coastal water of the NEAS during the NEM (av. $784 \pm 106 \text{ mgC m}^{-2} \text{ d}^{-1}$).

3.3.2. Phytoplankton size classes

3.3.2.1. Composition and abundance

The abundance of smaller plankton (nanoplankton, *Synechococcus*, and picoeukaryotes) was obtained from the group-specific clusters in the flow cytogram (Supplementary Figure 3). During the NEM, the total abundance of all phytoplankton size classes was higher in the surface waters of the NEAS compared to the SEAS, whereas such a clear spatial trend was not found in the subsurface waters (30 m), especially in the offshore waters (Figure 10). The total picoplankton abundance in the

entire EAS during the NEM, varied from $3 - 8.2 \times 10^6 \text{ L}^{-1}$ at the surface and $3 - 5.5 \times 10^6 \text{ L}^{-1}$ at the subsurface (Figure 10). The abundance of picoeukaryotes and *Synechococcus* were found only marginally lower in the offshore (av. $2.4 \pm 0.9 \times 10^6 \text{ L}^{-1}$ and av. $3.5 \pm 1.1 \times 10^6 \text{ L}^{-1}$, respectively) compared to the coastal waters (av. $2.5 \pm 0.6 \times 10^6 \text{ L}^{-1}$ and av. $3.6 \pm 0.9 \times 10^6 \text{ L}^{-1}$, respectively). During the NEM, the abundance of nano- and micro- plankton was more than a fold higher in the coastal waters of the NEAS compared to the SEAS (Figure 10). But such a prominent difference in the abundance of nano- and micro- plankton was not evident in the offshore waters of the NEAS and SEAS. The FlowCAM data showed that the microphytoplankton community was dominated by diatoms and dinoflagellates (Table 2). The diatoms were composed of 20 genera, which include *Chaetoceros*, *Coscinodiscus*, *Dictyocha*, *Heliotheca*, *Hemiaulus*, *Hemidiscus*, *Navicula*, *Nitzschia*, *Odontella*, *Planktionella*, *Pleurosigma*, *Pseudo-Nitzschia*, *Rhizosolenia*, *Thalassionema*, *Thalassiosira* (Table 2; Supplementary Figure 4). The dinoflagellates were composed of *Ceratium*, *Dinophysis*, and *Gymnodinium*

During the SWM, the most striking feature was the overall increase in the abundance of all the phytoplankton size classes in the coastal waters of the entire EAS. Among the NEAS and the SEAS, the latter region had a significantly higher abundance of all phytoplankton size classes. Similar to the NEM, all phytoplankton size classes during the SWM also showed their higher abundance in the surface waters compared to the subsurface (30m). During the SWM, the total picoplankton abundance in the entire EAS varied from $1.9 - 8.7 \times 10^6 \text{ L}^{-1}$ in the surface and $1.9 - 6.6 \times 10^6 \text{ L}^{-1}$ in the subsurface (Figure 10). The abundance of pico- and nano- plankton was higher in the coastal waters of the SEAS (av. $5.27 \pm 0.96 \times 10^6 \text{ L}^{-1}$ and $7.78 \pm 3.53 \times 10^6 \text{ L}^{-1}$, respectively) than in the coastal waters of the NEAS (av. $3.07 \pm 1.31 \times 10^6 \text{ L}^{-1}$ and $3.95 \pm 2.9 \times 10^6 \text{ L}^{-1}$, respectively), while such a clear trend was not found in the offshore region (Figure 10). The entire coastal waters of the EAS showed higher microphytoplankton abundance with a several-fold increase in the coastal waters of the SEAS (av. $5.79 \pm 1.15 \times 10^3 \text{ L}^{-1}$) compared to the NEAS (av. $1.92 \pm 2.12 \times 10^3 \text{ L}^{-1}$). As in the case of NEM, the microphytoplankton during the SWM was mainly composed of diatoms and dinoflagellates, with a significantly increased abundance of diatoms *Coscinodiscus*, *Thalassionema*, *Thalassiosira* and *Rhizosolenia* (Table 2). The dinoflagellates were composed of *Ceratium*, *Dinophysis*, and *Protoperdinium*. A striking feature in the nearshore waters during the SWM was the notable increase in colonies/long chains of some of the diatoms, such as *Thalassiosira* (> 8 cells/colony), *Thalassionema* (> 10 cells/colony), and *Asterionellopsis* (> 5 cells/colony). Overall, during the SWM, many-fold higher abundance of micro-and nano-phytoplankton was found in the nearshore waters of the EAS, especially in the SEAS.

3.3.2. 2. Size fractionation of Chl-a biomass

During the NEM, the overall integrated Chl-a was relatively high in the NEAS (av. 21.06 ± 8.24 mg m⁻²) than that in the SEAS (av. 11.88 ± 7.09 mg m⁻²) (Table 1). In the entire EAS, the column Chl-a during the NEM was dominantly contributed by nanoplankton (av. $68.1 \pm 8.7\%$) followed by microplankton (av. $9.2 \pm 11\%$). The nanoplankton biomass was dominant (av. 13.92 ± 5.01 mg m⁻²) and it contributed the maximum (av. $64.8 \pm 13.8\%$ of total Chl-a) to the total Chl-a even in NEAS, which had relatively more concentration of nutrients. This enhancement of nanoplankton biomass was consistent both in the coastal (av. $62.9 \pm 12.9\%$ of total Chl-a) and offshore (av. $69.9 \pm 8.9\%$ of total Chl-a) regions of the NEAS (Supplementary Figure 5). The vertical distribution of Chl-a biomass of phytoplankton size classes in the NEAS during the NEM also revealed nanoplankton to be the most abundant plankton fraction in the water column, particularly in the upper 60m, followed by microplankton (Figure 11). But, across the entire water column, the Chl-a biomass of these prominent phytoplankton size fractions did not exceed 0.5 mg m⁻³ (Figure 11). Also, the microplankton and nanoplankton were mostly restricted to the NEAS upper 60m water layer, but the noticeably low picoplankton Chl-a biomass was dispersed almost uniformly throughout the entire water column. Most notably, during the NEM, the largest size fraction (mesoplankton) of the chain-forming species was present at a relatively low level throughout the EAS (Figure 11).

In the EAS, the SWM showed the highest column Chl-a (avg. 41 ± 29.8 mg m⁻²) (Figure 9). It was very high at T1 station 4 (125.8 mg m⁻²). Microplankton (av. 48.1%) was the most dominant size fraction in the EAS inshore region at that time, with a higher contribution in the SEAS (av. $50.2 \pm 7.4\%$) than in the NEAS (av. $44.4 \pm 17.2\%$) (Supplementary Figure 5). However, the offshore region was dominated by more nanoplankton (av. 13 ± 3.3 mg m⁻²) contributing $61.8 \pm 13.6\%$ of the total Chl-a biomass (Table 1, Supplementary Figure 5). During this period, the nanoplankton contribution in the SEAS offshore (av. 13.93 ± 3.55 mg m⁻²) was slightly higher than the NEAS offshore (av. 11.52 ± 2.5 mg m⁻²) (Table 1). This period also evidenced a noticeably high contribution of mesoplankton to the total Chl-a (av. 8.56 ± 6.5 mg m⁻²), especially in the coastal region of the SEAS (av. 9.1 ± 4 mg m⁻²) (Figure 12). These indicate a greater influence of the SWM in favouring larger (meso- and micro-) plankton in the entire EAS. The vertical distribution of Chl-a biomass during the SWM revealed certain specific characteristics that are different from the NEM (Figure 12). The vertical biomass distribution of the meso, micro, and nanophytoplankton was fairly equally distributed throughout the upper 60 m water column during the NEM, whereas it was more limited to a considerably shallower upper water column during the SWM (30 m). Furthermore, the high concentration of Chl-a biomass of meso, micro,

and nanoplankton in the shallow surface layers of the coastal zone often extends and tapers towards the offshore in a tongue-like shape (Figure 12).

3.3. Ecological linkages

The result of multivariate RDA analysis is presented as Triplots (Figure 13), while the multiple correlations between parameters and their statistical significance are furnished in Supplementary Table 1. Triplots demarcate the seasonality in the hydrography with corresponding variations in the biological variables both in the NEAS and SEAS during the NEM and the SWM. During the NEM (Figure 13a), the SEAS is represented by the 3rd and 4th quadrants, where the waters are warm (SST arrow oriented towards the left side down) and nutrient-depleted (absence of nutrients). The parameter arrow of picoplankton was closely aligned with SST and directed towards the SEAS. This indicates that the nano size fraction of the phytoplankton is more favoured by the extreme oligotrophy of the SEAS during the NEM. Similarly, the NEAS is represented by the 1st and 2nd quadrants in the plot where it has relatively high nutrients (NO_3 , PO_4 and SiO_4) and is positively correlated with micro and meso- plankton (oriented towards the right-side-up). This infers that increasing nutrient enrichment in the cooler coastal euphotic zone in the NEAS is favourable for the growth of both micro and meso- plankton during the NEM. It must also be noted that the nanoplankton (in the centre only) did not show any specificity either in the SEAS or NEAS during NEM, which indicates that they are successful in survival in the entire EAS with varying nutrient regimes. The mesoplankton seems to proliferate in a nitrogen-rich environment with a high N/P ratio, whereas the microplankton shows a relative preference for a silica-rich environment with a high Si/N ratio.

The RDA results for the SWM shows the interaction of nutrients and their impact on structuring the different size classes of the phytoplankton. Importantly, there is no clear demarcation of the study region into the NEAS and SEAS, as all the 6 transects are scattered over the Triplot (Figure 13b). However, based on the nutrient distribution, a better classification for the period could be the coastal and offshore environment. Thus, it is evident that the entire coastal environment of the EAS is falling on the right side of the plot, where the major influencing factor is the nutrients (N, P and Si). On the left side, there is only one factor, represented by SST, which represents the offshore surface waters. Thus, the cooling associated with nutrient enrichment is due to intense upwelling over the entire coastal environment, while the offshore environment remained relatively warmer and nutrient-deplete. The stronger injection of nutrients especially in the SEAS is more evident in the clustering of all nutrient arrows. More significantly, the N/P and Si/N have moved closer indicating a uniform enrichment of both N and Si (significant correlation with nutrients; Supplementary Table 1). This is the conducive environment that supports the growth of both micro-and meso- plankton biomass. Here also, it can be

seen that mesoplankton prefers a relatively nitrogen-rich environment (N/P ratio), whereas microplankton prefers a silicon-rich environment (Si/N ratio). The offshore surface waters (left side of the plot) were relatively warmer (SST) and nutrient deficient during this period, which consequently favoured the growth of nano- and pico- plankton (significant correlation with SST). The RDA results infer that while nutrient-rich (cooler) condition is suitable for meso-/ micro- plankton and the nutrient-depleted (warmer) condition is suitable for the growth of picoplankton, the intermediate stage of nutrient-deficiency can be a stage where nanoplankton is preferably grown.

4. Discussion

4.1. Ecological effects of winter convection and coastal upwelling in the EAS

The phytoplankton bloom in the northern Arabian Sea during the NEM was first studied by Banse and McClain (1986), and now it is well well-known as a biological manifestation of the nutrient enrichment of the convective mixing (Madhupratap et al., 1996; Levy et al., 2007; Jyothibabu et al., 2010; Vijith et al., 2016). The OMZ in the northern Arabian Sea was partly explained by the occurrence of a large winter phytoplankton bloom there (Naqvi, 1987; Naqvi et al., 1982; 2002; Madhupratap et al., 1996, Jyothibabu et al., 2010). However, the shift of OMZ to the EAS was only recently explained (McCreary et al., 2013; Acharya and Panigrahi, 2016; Schmidt et al., 2019; Shenoy et al., 2020; Sarma et al., 2020). Low SST (25°C), high salinity (salinity > 36), and moderate to strong north-easterly winds (> 5 m s⁻¹) are typical winter convection conditions in the northern Arabian Sea, which were also observed in this study. However, it is worth noting that the geographical domain studied in this study was substantially smaller than previous winter convective investigations in the area (Madhupratap et al., 1996; Prasannakumar et al., 2001). During the current study, MLD in the NEAS was low in the shallow regions (av. 33.75 ± 13.83 m) and was high in the offshore areas (av. 52.88 ± 23.75 m), which could be attributed to the relatively high saline water mass in the latter region conducive for the vertical convection.

Though the nutrient enrichment associated with the winter convection and its impact on increasing the phytoplankton production in the northern Arabian Sea is well documented, the integration of its varying impacts on the phytoplankton community in the western, central, and eastern Arabian Seas has been accounted for at a minimal level, with the Indian shelf waters being almost ignored (Banse and McClain., 1986; Levy et al., 2007). Vijith et al., (2016) showed that the presence of low salinity warmer waters brought by the poleward West India Coastal Current inhibits the deepening of the mixed layer in the southern parts of the NEAS, resulting in a low concentration of nutrients and Chl-a biomass. However, in the current study, the overall nutrient content of the NEAS during the NEM was

moderate in the oceanic waters ($\text{NO}_3 - 0.62 \pm 0.45 \mu\text{M}$; $\text{SiO}_4 - 3.01 \pm 0.83 \mu\text{M}$ and $\text{PO}_4 - 0.49 \pm 0.13 \mu\text{M}$) while an enriched condition was found in the coastal waters ($\text{NO}_3 - 5.04 \pm 4.77 \mu\text{M}$; $\text{SiO}_4 - 10.49 \pm 7.89 \mu\text{M}$ and $\text{PO}_4 - 1.02 \pm 0.30 \mu\text{M}$). According to Banse and Postel (2009), winter convection is often limited to 21- 23°N, where primary productivity is higher than at lower latitudes. However, many subsequent studies showed vertical convection and nutrient enrichment even at much lower latitudes in the northern Arabian Sea during winter, and that too throughout the NEM, by vertical mixing of nutrient-rich waters from the mixed layer's base (50 - 120 m). However, as previously indicated, phytoplankton biomass is substantially larger in the western Arabian Sea than in the EAS, where Chl-a is moderate (Banse and McClain, 1986; Levy et al., 2007; Jyothibabu et al., 2010). The current study also found that during the peak winter convection phase, the oceanic northeastern Arabian Sea had low to moderate Chl-a levels at the surface (av. $0.38 \pm 0.11 \text{ mg m}^{-3}$) as well as in the entire euphotic column (av. $20.23 \pm 6.08 \text{ mg m}^{-2}$).

Several researchers attempted to explain the comparatively low amount of Chl-a in the NEAS winter convective zone, proposing the potential of a silicate limitation rather than a nitrate limitation for diatoms (Sawant and Madhupratap., 1996; Naqvi et al., 2002; Balachandran et al., 2008; Sarma et al., 2019), which is a typical characteristic of open-ocean upwelling systems (Dugdale and Goering., 1967; Dugdale and Wilkerson., 1992, 1998). The nutrient data from the current study, however, do not support a silicate limitation as a reason for the low/moderate level of Chl-a, as significantly enriched silicate levels were observed in the winter convective region (offshore $\text{SiO}_4 - 3.01 \pm 0.83 \mu\text{M}$ and coastal $\text{SiO}_4 - 10.49 \pm 7.89 \mu\text{M}$). Kumar et al., (2010) also observed lower Chl-a ($0.24 - 0.76 \text{ mg m}^{-3}$) and NO_3 uptake ($2.3 \text{ mmolN m}^{-2} \text{ d}^{-1}$) by phytoplankton during the peak winter convection in December than during late winter convection in February-March (NO_3 uptake of $12.7 \text{ mmolN m}^{-2} \text{ d}^{-1}$ and Chl-a $0.08 - 1.6 \text{ mg m}^{-3}$) and their nutrient data also did not support the view of a possible silicate limitation. On the other hand, they looked into the region's iron deficiencies in search of an explanation for the low NO_3 uptake by phytoplankton during the NEM, however, the high amounts of iron in the study region during the NEM contradicted the above reasoning.

A very recent study also looked into the aspect of Chl-a biomass and nutrient levels in the NEAS during the NEM (Lakshmi et al., 2021). Despite moderate NO_3 concentrations in the water column, they obtained low Chl-a in the NEAS ($0.1 - 0.3 \text{ mg m}^{-3}$), as was the case in Indian JGOFS data from the 1990s as well (Chl-a was $< 0.3 \text{ mg m}^{-3}$ at locations J5 to J8 in the NEAS; Bhattathiri et al., 1996). However, it is clear from Bhattathiri et al., (1996) that the high NO_3 concentration, which was expected in the NEAS, was not found consistently in all the locations and, out of 4 locations studied, two of them (J6 and J8) had a very trace level of NO_3 in the upper euphotic column. Lakshmi et al.,

(2021) have attempted the question of why Chl-a concentration in the NEAS is low during the NEM when vertical convection is operational there. They provided an explanation based on the fact that, apart from the nutrients, light plays an important role in defining the water column Chl-a and proposed that Sverdrup's critical depth hypothesis could be applicable in the NEAS during the NEM. And they propose that a deeper MLD (av. 60 m), a shallower euphotic column (av. 40m), and a low Si/DIN ratio (<1) could explain the observed low Chl-a in the NEAS during the NEM. But the current study does not support the above contention that a low euphotic column could limit the Chl-a biomass in the NEAS for the following logical reasons. (a) If solar radiation limitation is the case, naturally high Chl-a levels would be expected in the surface layers, which are nutrient-rich and well-lit for phytoplankton growth. But this is not the case in the NEAS during the NEM when Chl-a levels were significantly lower in the surface waters [$< 0.3 \text{ mg m}^{-3}$] -Bhattathiri et al. 1996; $(0.1 - 0.3 \text{ mg m}^{-3})$ -Lakshmi et al., 2021; $(\text{av. } 0.38 \pm 0.11 \text{ mg m}^{-3})$ - present study]. (b) the northwestern Arabian Sea, located at the same latitudes and exposed to similar solar radiation levels, shows a significantly higher concentration of Chl-a during the NEM through winter convection (Banse and McClain, 1986; Levy et al., 2007; Jyothibabu et al., 2010), (c) the past phytoplankton studies from the shelf waters of the southwest coast of India during the southwest monsoon do not support suggesting a light limitation of the phytoplankton in the NEAS during the NEM. Because the large diatom blooms on India's southwest coast occur during the peak and late SWM when euphotic depth is considerably lower ($<30\text{m}$) and the underwater light is significantly reduced due to increased turbidity and cloud cover (Karnan et al., 2017a; Jyothibabu et al., 2018b). It is noteworthy to consider here the observation of Kumar et al., (2010) that the vertically convected NO_3 in the NEAS had a longer residence period of more than 60 days during peak convection time in January, while it was shorter and less than 20 days during the late convection time in February and March. Their data suggested that unutilized NO_3 entrained in January could last into February and March, making it available for phytoplankton absorption. And this observation can more satisfactorily explain the prominent phytoplankton bloom that occurs in the NEAS during the late winter convection period in February-March (Banse and McClain, 1986; Levy et al., 2007; Jyothibabu et al., 2010; Lakshmi et al., 2021). From a biological standpoint, the low NO_3 uptake observed during peak convection in Kumar et al., (2010) suggests that the phytoplankton community present at that time was less efficient to assimilate the excess NO_3 inoculated in the enrichment experiments as quickly as the phytoplankton community of the late winter convection period. Unfortunately, this important ecological aspect was not discussed in Kumar et al., (2010).

Weak winds (av. $3.88 \pm 0.32 \text{ m s}^{-1}$), warm air (av. $26.32 \pm 0.82 \text{ }^\circ\text{C}$), high SST (av. $28.15 \pm 0.49 \text{ }^\circ\text{C}$), and low MLD (av. $27.8 \pm 4.6 \text{ m}$) were the characteristics of the SEAS during the NEM. Although

it was winter, enhanced solar heating (high SST) and the presence of low saline BoB waters on the surface were the causes of this state in the SEAS (Figure 2 & 3). The presence of low saline and warm BoB waters in the SEAS during the NEM was readily visible in satellite remote sensing data. During peak NEM, BoB waters occur even up to the southern section of the NEAS (Vijith et al., 2016; Shankar et al., 2019). Low saline, warm, and nutrient-poor waters eventually result in thermohaline stratification at the surface, resulting in low phytoplankton biomass (Jyothibabu et al., 2010). Low nitrate ($0.1 \mu\text{M}$) and phytoplankton biomass (0.2 mg m^{-3}) were observed in the SEAS during the NEM period of the current investigation. This oligotrophic state in the SEAS might last up to 8 months, from March to May and October to February (Jyothibabu et al., 2010). A notable exception was identified at the T1 transect, which was located 30 metres from the coast and had moderate phytoplankton biomass (0.3 mg m^{-3}), most likely due to advected waters from the Gulf of Mannar.

Studies on coastal upwelling in the EAS began in the 1950s (Ramasastry and Myrland, 1959; Banse, 1959). Subsequently, numerous scientists looked at the ecological aspects of coastal upwelling (Bhattathiri et al., 1996; Jyothibabu et al., 2008, 2010; Habeebrehman et al., 2008; Smitha et al., 2008; Gupta et al., 2016; Jagadeesan et al., 2017; Karnan et al., 2017a). Due to the orographic effect of the Western Ghats mountain, the oceanic southwesterly winds across the Arabian Sea are significantly transformed into westerly or northwesterly when they approach the Indian coastline during the SWM (Smitha et al., 2008; Hareeshkumar and Anand, 2016 and references therein). The shoaling of cool, oxygen-deficient and nutrient-rich deep waters towards the shelf is aided by the modified winds, resulting in coastal upwelling (Smitha et al., 2008; Hareeshkumar and Anand, 2016 and references therein). The vertical distribution of temperature, dissolved oxygen, and nutrients along all transects (T1 to T6) in the EAS during the SWM of the current study demonstrates clear upwelling signatures. The major signatures of coastal upwelling in the SEAS are the noticeable reductions in SST, subsurface DO, and a rise in all macronutrients, which can be traced even in very shallow waters close to the coastline (Banse, 1959; Gupta et al., 2016; Jagadeesan et al., 2017; Jyothibabu et al., 2021). Earlier research has demonstrated that coastal upwelling is critical in significantly increasing plankton productivity and associated fisheries along the western Indian coast (Banse., 1959; Jyothibabu et al., 2008, 2010; Habeebrehman et al., 2008; Gupta et al., 2016). Upwelling occurs along the west coast of India up to 16°N , after which it moves in a non-uniform manner (Banse., 1959; Shetye et al., 1990; Habeebrehman et al., 2008). The current study found that coastal upwelling occurs over the whole western shelf of the EAS, albeit at different intensities. The main causes of coastal upwelling are assumed to be local winds and remote forces through Kelvin and Rossby waves (Shetye et al., 1990; Smitha et al., 2008; Shalin and Sanilkumar, 2014; Hareeshkumar and Anand, 2016). The large extent

of nutrients carried by the upwelled water can have a significant impact on the quality and growth of phytoplankton in the nearshore seas (Karnan et al., 2017a). The nutrient-rich waters advected towards the coast during coastal upwelling originates from depths of 75 - 150 m in the offshore regions. The high concentration of nutrients advected/pumped by the upwelling becomes particularly significant in the thin surface mixed layers in the nearshore waters. A portion of these upwelled nutrient-rich waters carrying high phytoplankton biomass in the surface layers of the nearshore waters also spread offshore as surface plumes (Jyothibabu et al., 2010).

Essentially, nutrient enrichment and its translation into phytoplankton biomass have a certain time lag (Jyothibabu et al., 2008, 2010, 2018 a & b; 2021; Habeebrehman et al., 2008; Karnan et al., 2017a). Satellite remote sensing studies that address larger spatial scales have shown a lag of 1-2 months between the seasonal monsoonal forcing and the formation of phytoplankton blooms in the Arabian Sea (Bartolacci and Luther, 1999; George et al., 2012; Prakash et al., 2012; Shi and Wang., 2022). Experimental studies have shown that most phytoplankton species have a time lag varying from a few hours to a few days to respond to the nutrient enrichment depending on the species present (Collos, 1986; Jyothibabu et al., 2018). Coastal upwelling is believed to have three sequential phases with specific characteristics, which include (a) the initial phase when the cold, nutrient-rich subsurface waters come to the surface and initiate phytoplankton biomass build-up; (b) the productive or mature phase, characterised by the greatest accumulation of phytoplankton biomass; and (c) the relaxing phase, with decreased phytoplankton biomass due to dispersion and nutrient depletion (Barlow, 1982; Rodriguez et al., 1992; Habeebrehman et al., 2008). Many studies along India's southwest coast have found a one-month lag between the peak of phytoplankton biomass and its translation into the peak of zooplankton biomass during the upwelling phase (Madhuprathap et al., 1992; Jyothibabu et al., 2008; 2010; 2018a&b, 2021; MLR Plankton Atlas, 2011; Jagadeesan et al., 2017; Karnan et al., 2017a). On the other hand, the time lag between the physical mechanisms of upwelling, phytoplankton bloom formation, and the peak fish (Indian oil sardine) production along the southwest coast of India had been unaddressed until George et al. (2012), who showed a 2 to 3 month lag between phytoplankton bloom formation and a successful sardine fishery in the post-monsoon season. Similarly, Menon et al. (2019) presented the view that the classical match-mismatch hypothesis (Hjort 1914; Cushing 1974), which states that the survival rate of fish larvae is a function of the synchrony between the timing of hatching of eggs and the initiation of the seasonal phytoplankton bloom, holds good along the southwest coast of India as well, concerning the Indian oil sardine fishery. These observations could open the way for several future studies on ecosystem functioning and its effects on fishery production along India's west coast.

It was observed in many parts of the world that river influx inhibits coastal upwelling in the nearshore waters (Ramamirtham and Jayaraman, 1960; Duxbury, 1966; Bowden, 1984; Johns et al., 1993; Hickey et al., 2005; Tseng et al., 2014). It was found recently that the river influx in the nearshore waters along the west coast of India during the SWM may cause a low saline surface layer, capping the upwelling of cool, nutrient-rich waters in the nearshore region of the SEAS (Santhikrishnan et al., 2021). In the current study, low saline surface plumes were visible in some coastal locations in the SEAS during the SWM, especially at T2 adjacent to the Kochi backwaters that receive freshwater from seven rivers (Qasim, 2003). Hence, the Kochi coastal waters receive high loading of nutrients from the Kochi backwaters during the SWM (Jyothibabu et al., 2008; Madhu et al., 2010; 2017; Anjusha et al., 2018). It is very clear in the current study that Chl-a biomass in the entire EAS coastal waters was high during the SWM, which can be attributed to the combined effect of upwelling and river influx (Nair et al., 1992; Madhupratap et al., 1996; Bhattathiri et al., 1996; Jyothibabu et al., 2010; Shafeeque et al., 2019). However, while we have some satellite-based quantifications of rainfall in the research region, we still lack information on the cumulative nutrient impact via the discharges of the various rivers along India's southwest coast (Gupta et al., 2021). A summary of the processes that influence phytoplankton biomass production and distribution in the EAS is presented in Figure 14 (Madhupratap et al., 1996; Shetye et al., 2008; Jyothibabu et al., 2010) in the context of the inferences derived from the current study. The most important finding of this study is that physical mechanisms that cause considerable changes in space and time are important in structuring the level of phytoplankton biomass and their size classes in the EAS.

The presence of SCM is a consistent feature of stratified waters in the ocean (Sarma and Aswinikumar, 1991; Cullen, 2015 and references therein). Several reasons are attributed to the formation of SCM/DCM including an excitation in phytoplankton growth near the nutricline, enlargement of Chl-a pigments as a part of photoacclimation at depth, and changes in the buoyancy of phytoplankton that aggregates in layers to escape from being grazed (Cullen, 2015). The present study, however, shows the general absence of a well-defined SCM in the NEAS during the NEM or in the entire EAS shelf waters during the SWM. Alternatively, the SEAS during the NEM and the oceanic regions in the EAS during the SWM where the euphotic column was deep (>50m) and the nutrient concentrations in the upper euphotic column were low only showed the presence of SCM. It was observed earlier in the western Bay of Bengal that a shallow euphotic column in the continental shelf waters positions SCM at much shallower depths compared to the oceanic waters (Jyothibabu et al., 2018b). The winter convective zones of the northern Arabian Sea, according to Banse (1994), do not facilitate the formation of an SCM since the euphotic zone is shallower than the mixed layer at that

time. Many recent investigations (Kumar et al., 2010; Lakshmi et al., 2021), including this one, have found no SCM in the NEAS during the NEM. Bance's theory holds in the NEAS during the NEM, but not in the SEAS coastal waters during the SWM when the mixed layer was significantly shallower than the euphotic depth.

4.2. Nutrient limitations in the EAS

The generally accepted nutrient restriction hypothesis states that nitrogen (N) is the limiting nutrient for primary production in marine ecosystems, while phosphorus (P) plays a limiting role in lakes (Hecky and Kilham, 1988; Howarth and Marino, 2006). To identify nutrient limitations in natural phytoplankton communities, bioassays in which the phytoplankton community's reaction to N or P is assessed by introducing one or both nutrients in micro/mesocosms or inferred from elemental ratios are commonly used (Havens, 2000; Jane et al., 2008; Moreno and Martiny, 2018 and references therein). This is primarily because nutrient stoichiometry was found to be decisive in structuring the diatom community (Jane et al., 2008; Moreno and Martiny, 2018 and references therein). Although high nutrient load can result in increased algal biomass (Howarth, 1988; Beman et al., 2005), the relationship between nutrient load, phytoplankton stoichiometry and nutrient limitation are complex. Physiological studies have shown that plankton exhibit more dependence on the community response under the eutrophic condition as compared to the oligotrophic condition (Moreno and Martiny, 2018). In general, phytoplankton physiological nutrition requirements are species-specific (Quigg et al., 2003; Lagus et al., 2004).

The fundamental idea of rendering nutrient ratio for phytoplankton growth in Indian waters was discussed in Jane et al., (2008), showing that the atomic nitrate to silicate to phosphate (N: Si: P) ratio within diatom cells is roughly 16:16:1 when nutrition levels are sufficient for optimal growth (Redfield et al., 1963; Brzezinski, 1985). Nutrient availability or uptake deviations from these ratios suggest the possibility of nutrient-limited phytoplankton development (Hecky and Kilham, 1988; Dortch and Whitley, 1992). However, when the ambient ratios of dissolved N: P < 10 and N: Si ratio < 1, it indicates a potential N limitation, whereas N: Si > 1 and Si:P < 3 indicate a potential Si limitation (Harrison et al., 1977). Based on the above criteria, the nutrient ratios in the current study area shows the following interesting features. During the NEM, both the coastal and oceanic regions of the SEAS and the oceanic waters of the NEAS were N-limited. On the other hand, during the SWM, the offshore regions of the NEAS were SiO₄ limited (Table 1).

4.3. Responses of phytoplankton size classes to varying nutrient levels

The thumb rule evolved out of studies on marine phytoplankton size classes states that smaller plankton (pico and nano) dominate in oligotrophic conditions, whereas larger plankton (micro and meso) dominate in nutrient-rich conditions (Sieburth et al., 1978; Azam et al., 1983; Chisholm 1992; Maranon et al., 2009; Karnan et al., 2017a, b; 2020). It is well known that smaller sized phytoplankton has a key role in sustaining the microbial food web in the oligotrophic ocean (Gallegos et al., 1996; Quinlan et al., 2009; Robin et al., 2013). The responses of phytoplankton size classes to the physicochemical changes in the upper euphotic column are represented in Figure 14. The NEAS was moderately productive (Chl-a 6.9 - 41mg m⁻² and PP 237 - 889 mgC m⁻²) during the NEM, while the SEAS was oligotrophic (Chl-a 3.5 - 28.2 mg m⁻² and PP 113 - 252 mgC m⁻²) during the period. Usually, nutrient enrichment associated with physical processes favours the growth of large (meso and micro) phytoplankton (Subramanyam, 1959; Jyothibabu et al., 2015; Karnan et al., 2017 a, b). However, in the winter convection zone of the NEAS, the smaller (nano) plankton responded to the moderate nutrient enrichment and contributed significantly to the total Chl-a biomass (Figure 10 & 11). The analyses of the nutrient ratio suggested that the oceanic NEAS during the NEM was N-limited and, naturally, such a situation does not favour large micro- and meso-plankton communities as their nitrate requirements are significantly higher (Landry et al., 1998; Karnan et al., 2017 a, b). A similar observation of a significantly higher nanoplankton contribution was observed in the winter convection regions of the northwestern Mediterranean Sea (Leblanc et al., 2018). This study was based on the analysis of Tara Oceans data, together with a literature review, and indicated a general oversight of the significance of nanoplankton diatoms on a global scale (Leblanc et al., 2018). This study further showed that nanoplankton can reach the seafloor at high sinking rates, proposing a revision of the traditional/classical belief that only microphytoplankton sustain secondary trophic levels and vertical carbon export into the deep ocean layers (Leblanc et al., 2018).

Larger centric and chain-forming diatoms constitute the micro and meso-phytoplankton communities in the nutrient-rich upwelled waters of the EAS (Nair and Subrahmanyam., 1955; Nair et al., 1992; Karnan et al., 2017a, b; Jyothibabu et al., 2018). As mentioned before, the moderate nutrient enrichment generated by convective mixing could explain the low abundance of larger phytoplankton in the NEAS during the NEM. As indicated previously, the enrichment of micronutrients (NO₃, PO₄ and SiO₄) in the oceanic winter convective zones of the NEAS was significantly lower than in the upwelling regions of the EAS during the SWM. Several researchers have emphasised occurrences of SiO₄ limitation rather than nitrate limitation in diatoms in the NEAS during the NEM (Sawant and Madhupratap., 1996; Naqvi et al., 2002; Balachandran et al., 2008; Sarma et al., 2019). However, as

mentioned before, silicate concentrations in the NEAS found in the current study was well above the limiting levels. As a result, these conditions in the NEAS favoured the sustenance of nanoplankton rather than large micro and mesoplankton as observed elsewhere in the world (Dortch and Whittedge., 1992; Leblanc et al., 2018). The SEAS during the NEM, on the other hand, was oligotrophic (Chl-a 3.5 - 28.2 mg m⁻² and PP 113 - 252 mgC m⁻² d⁻¹) due to high surface layer stratification caused by the presence of warmer and less saline BoB waters, which favoured the growth of smaller size classes dominated by nanoplankton in the chl-a biomass (Figure 10 & 11).

The current observations (Figure 12) corroborate the earlier studies that showed the high abundance of micro and meso phytoplankton in the SEAS as a result of coastal upwelling (Nair and Subrahmanyam., 1955; Nair et al., 1992; Banse et al., 1996; Karnan et al., 2017a). Larger sized phytoplankton responds efficiently to the significant nutrients enriched conditions by growing in huge masses (Landry et al., 1998; Karnan et al., 2017a, b; Jyothibabu et al., 2018). This is the typical case of shelf waters of the SEAS during the SWM, where massive blooms of large chain-forming phytoplankton occur (Nair and Subrahmanyam., 1955; Nair et al., 1992; Banse et al., 1996; Karnan et al., 2017a, b). The nutrient ratios considered in the present study show that there were no limitations on N and Si in the entire EAS during the SWM except in the offshore regions of the NEAS, where a SiO₄ limitation was prevailing. But it was evident that the offshore regions of SEAS also had a significantly lower concentration of all nutrients compared to the shelf waters, but still supported the growth of smaller nanoplankton. This implies that the nutrient requirements of nanoplankton are much lower than those of micro- and mesoplankton, enabling their sustenance even in regions with moderate/low nutrient levels. It also implies that more than the nutrient ratio, the absolute concentrations of nutrients could also determine the structure of the phytoplankton size in these environments. This seems to be valid over the seasons also in the EAS, as the mixed layer nutrient enrichment (especially N and Si) during the upwelling in the SEAS was several fold higher compared to that during the convective mixing in the NEAS. This probably resulted in a significant increase in overall phytoplankton biomass, with micro- and mesoplankton dominating in the SEAS shelf waters during the SWM and nanoplankton dominating in the whole NEAS including the winter convection zones during the NEM (Banse., 1959; Habeebrehman et al., 2008; Vijayan et al., 2021). In this line, the observation of Kumar et al., (2010) that high NO₃ assimilation of phytoplankton during the late NEM is also explainable as a result of an increased abundance of the larger diatom community during that period, which is usually characterised by significantly higher Chl-a biomass and the existence of larger diatom blooms (Banse and McClain, 1986; Levy et al., 2007; Jyothibabu et al., 2010; Lakshmi et al., 2021).

In the oceanic regions of the NEAS, vertical mixing erodes the base of the mixed layer (usually 50 - 120 m) and, as a result, the silicicline, which is located much deeper in the water column, is excluded from the mixing process. Also, the newly available nutrients through eroding the base of the mixed layer gets uniformly mixed/available in a relatively deep mixed layer, which causes only a moderate increase in their concentration in the water column. On the other hand, in the SEAS, the upwelling brings/adveacts nutrient-rich waters from a much deeper depth (75 - 150 m) to a shallow mixed layer in the nearshore waters and the magnitude of this enrichment is much higher than that present in the NEAS during the winter convective time. It was observed recently that the most significant primary response of the microphytoplankton to the coastal upwelling associated eutrophication is an increase in their mean bio-volume, either by increasing the individual cell size or by forming large colonies (Jyothibabu et al., 2021). The colony-forming habits of many diatoms in coastal upwelling regions, also observed in the present study, can be considered as a typical biological response of these diatoms to significantly high nutrient levels in these regions (Jyothibabu et al., 2021). The EAS nearshore waters are believed to receive a high concentration of N and Si from river influx during the SWM, but focused studies are needed to quantify the magnitude of riverine contribution to nutrient enrichment (Jyothibabu et al., 2010; Gupta et al., 2021).

McCarthy et al., (1999) observed a synchronous balance between new and regenerated production in the NEAS during winter, sustaining a consistent f-ratio even when the nitrate supply was high. This was further verified by another study in the NEAS during winter, where the regenerated production supported the growth of both mixotrophic dinoflagellates and smaller plankton (Dugdale and Goering, 1967; Prasannakumar et al., 2010). Studies have also shown that large meso and microplankton grow profoundly under eutrophic or mesotrophic conditions (Chisholm 1992; Banse et al., 1996; Guenther et al., 2015; Karnan et al., 2017a, b; 2020; Gauns et al., 2020). In the current study, during the NEM, the NEAS euphotic column was moderately rich in nutrients, though the proliferation of larger micro and mesoplankton was relatively low as compared to the upwelling region of the SEAS. Studies in diverse marine environments world over show that nannoplankton is responsible for 80 - 99% of phytoplankton production (Ryther, 1969; Gilmartin, 1964; Malone, 1971 and references therein; Leblanc et al., 2018). The dominance of nanoplankton in the total phytoplankton biomass in the estuarine and coastal environments along the eastern Arabian Sea has been noticed in many studies (Madhu et al., 2010; Jyothibabu et al., 2015; Anjusha et al., 2018). Though the smaller plankton biomass also increases during the seasonal nutrient enrichment during the SWM, their biomass production remains much slower than the larger phytoplankton (Banse et al., 1996; Agawin et al., 2000; Karnan et al., 2017a).

The classical microscopy studies of phytoplankton have varying observations in the NEAS. Studies associated with Indian JGOFS in the 1990s reported the predominance of diatoms (Sawant and Madhupratap; 1996), whereas, a more recent study with a more intensive and high-resolution monthly sampling during the NEM showed the predominance of *Trichodesmium* and diatoms (Matondkar et al., 2007). But essentially, these microscopic studies addressed the microplankton community in the study area since the phytoplankton <20µm size (nano- and pico) are unable to be accounted for in traditional microscopical methods. The microplankton analyses in the current study using a Flow Cam also showed the predominance of diatoms in the study area. The results of the current study showed that the micro and mesoplankton contribution to the phytoplankton Chl-a biomass changed from a considerable level in the EAS shelf waters during the SWM to a reduced level in the offshore waters and throughout the entire EAS during the NEM. The data sets of this study also, similar to Roy et al., (2015) and Rao et al., (2018), have signatures of the widespread occurrence of the picoplankton community in the entire EAS with an increase in the offshore waters, but their contribution to the total phytoplankton Chl-a biomass never found to exceed that of the micro-and mesoplankton in the upwelling regions and nanoplankton in the entire study region regardless of seasons.

One aspect which is lacking in the current study is information about the composition of the nanophytoplankton community in the EAS, which is beyond the reach of the methodologies used in this study. Specific studies on the composition of the nanophytoplankton community world over are very scarce (Tilstone et al., 1999; Leblanc et al., 2018). Tilstone et al., (1999) showed that the nanophytoplankton community in the coastal upwelling regions of NW Spain was mainly composed of smaller diatoms and flagellates, whereas Leblanc et al., (2018) in the northwestern Mediterranean Sea showed the predominance of smaller diatoms like *Minidiscus* in the nanoplankton size class. It is noteworthy to mention that the observations of Tilstone et al., (1999) in the NW Spain on the pattern of dominance of the different phytoplankton size classes to the nutrient enrichment associated with coastal upwelling was very similar to the observations in the present study. Therefore, it is very relevant to have detailed future studies on the composition of the nanophytoplankton community thriving in the different environmental settings in the EAS to understand the ecosystem ecology with further clarity.

4.4. Bottom-up and top-down controls on phytoplankton

The phytoplankton productivity cycles in marine environments are controlled by two major factors, such as the bottom-up by nutrients and the top-down by herbivory (Metaxas and Scheibling, 1996). The relative dominance of these two controls determines the type and stock of phytoplankton proliferating in an environment (Kerfoot and Sih 1987 and references therein). Many studies have

shown top-down as an important factor in defining phytoplankton biomass and size (Lynch and Shapiro 1981; Carpenter and Kitchell 1984, Vanni and Findlay 1990, Hansson 1992). Some other studies show that top-down control (zooplankton grazing) may not be efficient in controlling the phytoplankton growth (Threlkeld 1988; McQueen et al. 1989; Hansson 1992). The relative importance of bottom-up and top-down controls during each season is attributable to the establishment of alternate food chains including herbivore/omnivore/carnivore (Vanni 1987, Vanni and Temte 1990, Hansson, 1992). The nutrient uptake by phytoplankton and their transfer to higher trophic levels through grazing have been so far considered, though their relative importance (bottom-up and top-down controls) is pertinent seasonally (Wassman 1991; Kivi et al., 1993). Thus, it can be deduced that the more intense eutrophic conditions of upwelling along the entire EAS favoured high growth of micro and mesoplankton, favouring a short herbivorous food chain (Pomroy 1974; Azam et al., 1983; Cury et al., 2000; Landry et al., 2002; Irwin et al., 2006).

The larger diatoms that are abundant in the nearshore waters of EAS quickly consume the enriched nutrients during the SWM (Subrahmanian, 1959; Nair et al, 1992; Landry et al., 1998). Landry et al., (1998) observed that the phytoplankton community in the coastal upwelling areas has a much higher growth rate (0.9 to 2.2 d^{-1}) compared to the nutrient impoverished regions ($<0.5 \text{ d}^{-1}$). The widespread blooming of larger diatoms (*Fragilaria*, *Coscinodiscus*, and *Chaetoceros*) in the SEAS can be attributed to bottom-up control (Nair and Subrahmanyam, 1955; Nair et al., 1992; Jyothibabu et al., 2010; Karnan et al., 2017a). The possible role of top-down control of the phytoplankton biomass of large diatoms in the nearshore waters of the EAS was first presented by Banse et al., (1996). This study and Jagadeesan et al., (2017) presented the view that the inefficient grazing of copepods on larger diatoms makes them less competent to control diatom blooms, and hence, such blooms prevail along the nearshore waters of the EAS during the SWM. The experimental study of Jagadeesan et al., (2017) showed that the dominant copepods in the nearshore waters of the SEAS are small in size and, therefore, they are unable to efficiently graze and control the micro phytoplankton blooms. Instead, these smaller copepods in the EAS prefer to feed on the nano-size fraction of the phytoplankton community and exert more top-down control over them. In a similar line, studies elsewhere also showed that calanoid copepods are more selective during high concentrations of food and they preferably feed on $5 - 25 \mu\text{m}$ cells (Paffenhofers et al., 1982; Price et al., 1983; Tackx et al., 1989; Sautour et al., 2000; Lee et al., 2012). Evidence is also available from the SEAS and many other parts of the world that calanoid copepods have a negative selection preference for picoplankton fractions (Paffenhofers et al., 1982; Price et al., 1983; Sautour et al., 2000; Jagadeesan et al., 2017).

Another possible top-down control of larger diatoms in the nearshore waters of the EAS is from the three commercially important planktivorous small pelagic fishes, such as Indian oil sardine, Indian mackerel, and anchovy. These three fishes contribute more than 70% of the pelagic fishery landings along the west coast of India. During the SWM, significantly high stocks of oil sardine, mackerel and anchovy, the major small planktivorous pelagic fish, occur along the west coast of India (Madhupratap et al., 2001). The feeding studies of these fishes show that oil sardines feed predominantly on phytoplankton, mackerel almost equally on phytoplankton and zooplankton, and anchovy strictly on zooplankton (Rykaczewski and Checkley Jr., 2008; Nair et al., 2016; Karnan et al., 2017). Cury et al., (2000) found that in upwelling ecosystems, there is often a crucial intermediate trophic level, occupied by small, plankton-feeding pelagic fishes dominated by one or a few schooling species. It is known that sardines, mackerel and anchovy do not occupy the same niche and they usually utilise resources available at different trophic levels. Therefore, the collective grazing pressure of these planktivorous fishes may not be sufficient enough to regulate the frequent diatom blooms occurring along the southwest coast of India during the SWM. On the other hand, the smaller copepods predominant in the EAS may exert a significant level of top-down control over the nanoplankton community through preferential grazing both in the upwelling zones during the SWM and in the winter convection zones during the NEM. Experimental quantification of the top-down control of copepods on nanoplankton and its seasonal dynamics in the EAS are important topics for future research.

5. Conclusion

Based on *in-situ* sampling during the SWM and NEM seasons, this study presents the response of phytoplankton size classes to seasonal variations in the hydrography of the EAS associated with coastal upwelling and convective mixing. The NEAS was moderately nutrient-rich during the NEM, and nanoplankton dominated the Chl-a biomass. The SEAS was oligotrophic during the NEM, with nano and picoplankton dominating the Chl-a biomass. The SEAS was extremely productive during the SWM, resulting in a massive proliferation of large meso and microplankton. During this period, the nearshore seas of the NEAS also showed nutrient enrichment and increased phytoplankton biomass, but to a lesser extent than the SEAS. Overall, winter convective mixing and coastal upwelling had different effects on phytoplankton size classes in the EAS. Upwelling favoured larger meso and micro-sized fractions, but convective mixing in the NEAS favoured nanoplankton dominance, all of which can be connected to the variations in the macronutrient concentrations caused by these physical processes. In the NEAS, convective mixing takes place within the upper 50–120 m, whereas nutrient-rich subsurface waters from 75–150 m offshore are advected to the shallow mixed layer in nearshore waters in the coastal upwelling region. This scenario results in moderate nutrient enrichment in the

winter convective zones of the NEAS during the NEM and significantly higher nutrient enrichment throughout the whole upwelling regions of the nearshore waters during the SWM. Similarly, river discharge may also contribute to the nutrient pool in the upwelling zones in the nearshore waters of the EAS during the SWM, but its direct quantification is currently lacking. The current study concludes that during the SWM, upwelling zones in the nearshore waters of the EAS are noticeably more conducive to the growth of larger meso- and micro-phytoplankton than the winter convective zones of the NEAS during the NEM. The contribution of nanophytoplankton to the total Chl-a biomass was the most dominant in all conditions except in the considerably nutrient-loaded shelf waters of the EAS during the upwelling, indicating their efficient survival even in nutrient constrained environments.

Acknowledgement

The authors acknowledge the Director, CSIR- National Institute of Oceanography, India for facilities and support. We thank Dr. M. Sudhakar, the former Director, Centre for Marine Living Resources and Ecology, and the Director, National Centre for Coastal Research, Chennai India for the great support and encouragement for the research programme MEDAS to which this study is associated. We acknowledge all participants of various MEDAS cruises and colleagues in the National Institute of Oceanography, India who helped in different stages of this work. This is CSIR-NIO and CMLRE contribution ---- and -----, respectively.

References

- Acharya, S.S., Panigrahi, M.K., 2016. Eastward shift and maintenance of Arabian Sea oxygen minimum zone: Understanding the paradox. *Deep-Sea Research Part I: Oceanographic Research Papers* 115, 240-252.
- Agawin, N.S.R., Duarte, C.M., Agusti, S., 2000. Nutrient and temperature control of the contribution of picoplankton to phytoplankton biomass and production. *Limnology and Oceanography* 45, 591-600.
- Ahmed, A., Kurian, S., Gauns, M., Chandrasekhara Rao, A.V., Mulla, A., Naik, B., Naik, H., Naqvi, S.W.A., 2016. Spatial variability in phytoplankton community structure along the eastern Arabian Sea during the onset of south-west monsoon. *Continental Shelf Research* 119, 30-39.
- Anjusha, A., Jyothibabu, R., Jagadeesan, L., 2018. Response of microzooplankton community to the hydrographical transformations in the coastal waters off Kochi, along the southwest coast of India. *Continental Shelf Research* 167, 111-124.
- Asha Devi, C.R., Jyothibabu, R., Sabu, P., Jacob, J., Habeebrehman, H., Prabhakaran, M.P., Jayalakshmi, K.J., Achuthankutty, C.T., 2010. Seasonal variations and trophic ecology of microzooplankton in the southeastern Arabian Sea. *Continental Shelf Research* 30, 1070-1084.
- Azam, F., Fenchel, T., Field, J.G., Gray, J.S., Meyer-Reil, L.A., Thingstad, F., 1983. The ecological role of water-column microbes in the sea. *Marine Ecology Progress Series* 257-263.

- Balachandran, K.K., Laluraj, C.M., Jyothibabu, R., Madhu, N.V., Muraleedharan, K.R., Vijay, J.G., Maheswaran, P.A., Ashraff, T.T.M., Nair, K.K.C., Achuthankutty, C.T., 2008. Hydrography and biogeochemistry of the northwestern Bay of Bengal and the northeastern Arabian Sea during the winter monsoon. *Journal of Marine Systems* 73, 76-86.
- Banse, K., Postel, J. R., 2009. Wintertime convection and ventilation of the upper pycnocline in the northernmost Arabian Sea. *Indian Ocean biogeochemical processes ecological variability. Geophysical Monograph Series* 185, 87–117 .
- Banse, K., 1959. On upwelling and bottom-trawling off the southwest coast of India. *Journal of the Marine Biological Association of India* 1, 33-49.
- Banse, K., 1994. On the coupling of hydrography, phytoplankton, zooplankton, and settling organic particles offshore in the Arabian Sea. *Proceedings of the Indian Academy of Sciences (Earth and Planetary Science Letters)*, Vol. 103, No. 2, June 1994, pp. 125-161.
- Banse, K., McClain, CR., 1986. Winter blooms of phytoplankton in the Arabian Sea as observed by the Coastal Zone Color Scanner. *Marine Ecology Progress Series* 201-211.
- Banse, K., Sumitra, V., Madhupratap, M., 1996. On the possible causes of the seasonal phytoplankton blooms along the southwest coast of India. *Oceanographic Literature Review* 6(44), 605-606.
- Barlow, R.G., 1982. Phytoplankton ecology to the Southern Benguela Current I Biochemical composition. *Journal of Experimental Marine Biology and Ecology* 63, 209–227.
- Bartolacci, D.M., Luther, M.E., 1999. Patterns of co-variability between physical and biological parameters in the Arabian Sea. *Deep-Sea Research II*, 46,1933-1964.
- Bemal, S., Anil, A.C., Amol, P., 2019. Picophytoplankton variability: Influence of Rossby wave propagation in the southeastern Arabian Sea. *Journal of Marine Systems* 199,103221.
- Bemal, S., Anil, A.C., Shankar, D., Remya, R., Roy, R., 2018. Picophytoplankton variability: Influence of winter convective mixing and advection in the northeastern Arabian Sea. *Journal of Marine Systems* 180, 37-48.
- Beman, J. M., Arrigo, K. R. and Matson, P.A., 2005. Agricultural runoff fuels large phytoplankton blooms in vulnerable areas of the ocean. *Nature* 434, 211–214.
- Bhattathiri, P.M.A., Pant, A., Sawant, S., Gauns, M., Matondkar, S.G.P., Mohanraju, R., 1996. Phytoplankton production and chlorophyll. *Current Science* 71(11).
- Binu, M.S., 2003. Studies on the fish larvae of the Arabian Sea with special reference to Clupeiformes. Ph.D thesis, Cochin University of Science and Technology, Kochi, India, pp. 240.
- Bowden, W.B., 1984. Nitrogen and phosphorus in the sediments of a tidal, freshwater marsh in Massachusetts. *Estuaries* 7, 108 -118.
- Brewin, R.J., Morán, X.A.G., Raitos, D.E., Gittings, J.A., Calleja, M.L., Viegas, M., Ansari, M.I., Al-Otaibi, N., Huete-Stauffer, T.M., Hoteit, I., 2019. Factors regulating the relationship between total and size-fractionated chlorophyll-a in coastal waters of the Red Sea. *Frontiers in microbiology* 10, 1964.

- Burson, A., Stomp, M., Greenwell, E., Grosse, J., Huisman, J., 2018. Competition for nutrients and light: testing advances in resource competition with a natural phytoplankton community. *Ecology* 99, 1108-1118.
- Carpenter, S.R., Kitchell, J.F., 1984. Plankton community structure and limnetic primary production. *American Naturalist* 124, 159-172.
- Chidambaram, K., Menon, M.D., 1945. The co-relation of the West Coast (Malabar & South Kanara) fisheries with plankton and certain oceanographical factors *Proceedings of the Indian Academy of Sciences-Section B*. Springer, 355-367.
- Chisholm, S.W., 1992. Phytoplankton size. In: *Primary productivity and biogeochemical cycles in the sea*. Springer, 213-237.
- Clarke, K.R., Warwick, R.M., 2001. A further biodiversity index applicable to species lists: variation in taxonomic distinctness. *Marine Ecology Progress Series* 216, 265-278.
- Collos, Y. 1986. Time-lag algal growth dynamics: biological constraints on primary production in aquatic environments. *Marine Ecology Progress Series* 33, 193–206
- Cullen, J.J., 2015. Subsurface chlorophyll maximum layers: enduring enigma or mystery solved?. *Annual Review of Marine Science* 7, 207-239.
- Cury, P., Bakun, A., Crawford, R.J.M., Jarre, A., Quinones, R.A., Shannon, L.J., Verheye, H.M., 2000. Small pelagics in upwelling systems: patterns of interaction and structural changes in wasp-waist ecosystems. *ICES Journal of Marine Science* 57, 603-618.
- Cushing, D.H., 1974. The natural regulation of fish populations. In: Harden Jones FR (ed) *Sea fisheries research*. Elek Science, London, 399-412.
- Cushing, D.H., 1989. A difference in structure between ecosystems in strongly stratified waters and in those that are only weakly stratified. *Journal of Plankton Research* 11,1-13.
- Department of Fisheries, 2020. *Handbook on Fisheries statistics*. Department of Fisheries Ministry of Fisheries, Animal Husbandry & Dairying Government of India, New Delhi, 196.
- Dortch, Q., Whitledge, T.E., 1992. Does nitrogen or silicon limit phytoplankton production in the Mississippi River plume and nearby regions?. *Continental Shelf Research* 12(11), 1293-1309.
- Dugdale, R., Wilkerson, F., 1992. Nutrient limitation of new production in the sea. In: *Primary productivity and biogeochemical cycles in the sea*. Springer, 107-122.
- Dugdale, R.C., Goering, J.J., 1967. Uptake of new and regenerated forms of nitrogen in primary productivity 1. *Limnology and oceanography* 12, 196-206.
- Dugdale, R.C., Wilkerson, F.P., 1998. Silicate regulation of new production in the equatorial Pacific upwelling. *Nature* 391, 270-273.
- Duxbury, A.C., 1966. The Union of the Columbia River and the Pacific Ocean: General Features. *Ocean Science and Ocean Engineering* 2, 914-922.

Gallegos, C.L., Vant, W.N., Safi, K.A., 1996. Microzooplankton grazing of phytoplankton in Manukau Harbour, New Zealand. *New Zealand Journal of Marine and Freshwater Research* 30, 423-434.

Garcia-Robledo, E., Corzo, A., Papaspyrou, S., 2014. A fast and direct spectrophotometric method for the sequential determination of nitrate and nitrite at low concentrations in small volumes. *Marine Chemistry* 162, 30-36.

Garrison, D.L., Gowing, M.M., Hughes, M.P., 1998. Nano-and microplankton in the northern Arabian Sea during the Southwest Monsoon, August-September 1995 A US-JGOFS study. *Deep-Sea Research Part II: Topical Studies in Oceanography* 45, 2269-2299.

Gauns, M., Mochamadkar, S., Pratihary, A., Shirodkar, G., Narvekar, P.V., Naqvi, S.W.A., 2020. Phytoplankton associated with seasonal oxygen depletion in waters of the western continental shelf of India. *Journal of Marine Systems* 204, 103308.

Gilmartin, M., 1964. The primary production of a British Columbia fjord. *Journal of Fisheries Research Board of Canada* 21, 505-538.

George, G., Meenakumari, B., Raman, M., Kumar, S., Vethamony, P., Babu, M.T., Verlecar, X., 2012. Remotely sensed chlorophyll: a putative trophic link for explaining variability in indian oil sardine stocks. *Journal of Coastal Research* 28, 105-113.

Grasshoff, K., Ehrhardt, M., Kremling, K., 1999. *Methods of Sea Water Analysis*, 3rd ed., Weinheim, New York, Wiley-VCH, pp. 75–89, 159–196.

Guenther, M., Araujo, M., Flores-Montes, M., Gonzalez-Rodriguez, E., Neumann-Leitao, S., 2015. Eutrophication effects on phytoplankton size-fractioned biomass and production at a tropical estuary. *Marine pollution bulletin* 91, 537-547.

Gupta, G.V.M., Sudheesh, V., Sudharma, K.V., Saravanane, N., Dhanya, V., Dhanya, K.R., Lakshmi, G., Sudhakar, M., Naqvi, S.W.A., 2016. Evolution to decay of upwelling and associated biogeochemistry over the southeastern Arabian Sea shelf. *Journal of Geophysical Research: Biogeosciences* 121,159-175.

Gupta, G. V .M., Jyothibabu, R., Ramu, Ch. V., Reddy, Y, A., Balachandran, K, K, Sudheesh, V., Kumar, S., Chari, N V H K., Bepari, K.F., Marathe, P. H., 2021. The world's largest coastal deoxygenation zone is not anthropogenically driven *Environmental Research Letters* 16 (5), 054009.

Habeebrehman, H., Prabhakaran, M.P., Jacob, J., Sabu, P., Jayalakshmi, K.J., Achuthankutty, C.T., Revichandran, C., 2008. Variability in biological responses influenced by upwelling events in the Eastern Arabian Sea. *Journal of Marine Systems* 74, 545-560.

Hansson, L.A., 1992. The role of food chain composition and nutrient availability in shaping algal biomass development. *Ecology* 73, 241-247.

HareeshKumar, P.V., Anand, P., 2016. Coastal upwelling off the southwest coast of India: observations and simulations. *International Journal of Digital Earth* 9, 1256-1274.

Harrison, P.G., 1997. Silicate cages: precursors to new materials. *Journal of Organometallic Chemistry* 542(2), 141-183.

- Havens, K.E., Hauxwell, J., Tyler, A.C., Thomas, S., McGlathery, K.J., Cebrian, J., Valiela, I., Steinman, A.D., Hwang, S.J., 2001. Complex interactions between autotrophs in shallow marine and freshwater ecosystems: implications for community responses to nutrient stress. *Environmental pollution* 113(1), 95-107.
- Hecky, R., Kilham, P., 1988. Nutrient limitation of phytoplankton in freshwater and marine environments: a review of recent evidence on the effects of enrichment. *Limnology and Oceanography* 33, 796-822.
- Hickey, B., Geier, S., Kachel, N., MacFadyen, A., 2005. A bi-directional river plume: The Columbia in summer. *Continental Shelf Research* 25, 1631-1656.
- Hjort, J., 1914. Fluctuations in the great fisheries of Northern Europe viewed in the light of biological research. *Rapports et procès-verbaux des reunions - International Council for the Exploration of the Sea* 20: 1–228.
- Howarth, R.W. (1988) Nutrient limitation of net primary production in marine ecosystems. *Annual Review of Ecology, Evolution, and Systematics* 19, 89–110.
- Howarth, R.W., Marino, R., 2006. Nitrogen as the limiting nutrient for eutrophication in coastal marine ecosystems: evolving views over three decades. *Limnology and Oceanography* 51, 364–376.
- Irwin, A.J., Finkel, Z.V., Schofield, O.M.E., Falkowski, P.G., 2006. Scaling-up from nutrient physiology to the size-structure of phytoplankton communities. *Journal of plankton research* 28, 459-471.
- Jagadeesan, L., Jyothibabu, R., Arunpandi, N., Karnan, C., Balachandran, K.K., 2017. Dominance of coastal upwelling over Mud Bank in shaping the mesozooplankton along the southwest coast of India during the Southwest Monsoon. *Progress in Oceanography* 156, 252-275.
- Jane, T.B., Ramaiah, N., Sardesai, S.R., 2008. Nutrient regimes and their effect on distribution of phytoplankton in the Bay of Bengal. *Marine Environmental Research* 66(3), 337-344
- Jiang, Z., Du, P., Liu, J., Chen, Y., Zhu, Y., Shou, L., Zeng, J., Chen, J., 2019. Phytoplankton biomass and size structure in Xiangshan Bay, China: current state and historical comparison under accelerated eutrophication and warming. *Marine Pollution Bulletin* 142, 119-128.
- Jiao, N., Ni, I.H., 1997. Spatial variations of size-fractionated chlorophyll, cyanobacteria and heterotrophic bacteria in the Central and Western Pacific Asia-Pacific Conference on Science and Management of Coastal Environment. Springer, 219-230.
- Johns, B., Rao, A.D., Dube, S.K., Sinha, P.C., 1993. The effect of freshwater discharge from the Godavari River on the occurrence of local upwelling off the East Coast of India. *Estuarine, Coastal and Shelf Science* 37, 299-312.
- Jyothibabu, R., Asha Devi, C.R., Madhu, N.V., Sabu, P., Jayalakshmy, K.V., Jacob, J., Habeebrehman, H., Prabhakaran, M.P., Balasubramanian, T., Nair, K.K.C., 2008. The response of microzooplankton (20–200 μm) to coastal upwelling and summer stratification in the southeastern Arabian Sea. *Continental Shelf Research* 28, 653-671.

- Jyothibabu, R., Madhu, N.V., Habeebrehman, H., Jayalakshmy, K.V., Nair, K.K.C., Achuthankutty, C.T., 2010. Re-evaluation of paradox of mesozooplankton in the eastern Arabian Sea based on ship and satellite observations. *Journal of Marine Systems* 81, 235-251.
- Jyothibabu, R., Vinayachandran, P.N., Madhu, N.V., Robin, R.S., Karnan, C., Jagadeesan, L., Anjusha, A., 2015. Phytoplankton size structure in the southern Bay of Bengal modified by the Summer Monsoon Current and associated eddies: Implications on the vertical biogenic flux. *Journal of Marine Systems* 143, 98-119.
- Jyothibabu, R., Arunpandi, N., Jagadeesan, L., Karnan, C., Lallu, K.R., Vinayachandran, P.N., 2018a. Response of phytoplankton to heavy cloud cover and turbidity in the northern Bay of Bengal. *Scientific Reports* 8, 1-15.
- Jyothibabu, R., Balachandran, K.K., Jagadeesan, L., Karnan, C., Arunpandi, N., Naqvi, S.W.A., Pandiyarajan, R.S., 2018b. Mud Banks along the southwest coast of India are not too muddy for plankton. *Scientific reports* 8, 1-13.
- Jyothibabu, R., Karnan, C., Jagadeesan, L., Arunpandi, N., Parthasarathi, S., Albin, K. J., 2021. Ecological responses of autotrophic microplankton to the eutrophication of the coastal upwelling along the Southwest coast of India. *Environmental Science and Pollution Research* 28(9), 11401-11414.
- Karnan, C., Jyothibabu, R., Arunpandi, N., Albin, K.J., Parthasarathi, S., Krishnan, S.S., 2020. Response of microplankton size structure to summer stratification, freshwater influx and coastal upwelling in the Southeastern Arabian Sea. *Continental Shelf Research* 193, 104038.
- Karnan, C., Jyothibabu, R., Arunpandi, N., Jagadeesan, L., Muraleedharan, K.R., Pratihari, A.K., Balachandran, K.K., Naqvi, S.W.A., 2017a. Discriminating the biophysical impacts of coastal upwelling and mud banks along the southwest coast of India. *Journal of Marine Systems* 172, 24-42.
- Karnan, C., Jyothibabu, R., Kumar, T.M.M., Balachandran, K.K., Arunpandi, N., Jagadeesan, L., 2017b. Seasonality in autotrophic mesoplankton in a coastal upwelling-mud bank environment along the southwest coast of India and its ecological implications. *Continental Shelf Research* 146,1-12.
- Kerfoot, W.C., Sih, A., 1987. Predation: direct and indirect effects on aquatic communities. University Press of NewEngland. Hanover, pp. 386.
- Kivi, K., Kaitala, S., Kuosa, H., Kuparinen, J., Leskinen, E., Lignell, R., Marcussen, B., Tamminen, T., 1993. Nutrient limitation and grazing control of the Baltic plankton community during annual succession. *Limnology and Oceanography* 38, 893-905.
- Kumar, S., Ramesh, R., Dwivedi, R. M., Raman, M., Sheshshayee, M. S., D'Souza, W., 2010. Nitrogen Uptake in the Northeastern Arabian Sea during Winter Cooling. *International Journal of Oceanography* 819029.
- Lagus, A., Suomela, J., Weithoff, G. Heikkilä, K., Helminen, H., Sipura, J., 2004. Species-specific differences in phytoplankton responses to N and P enrichments and the N : P ratio in the Archipelago Sea, northern Baltic Sea. *Journal of Plankton Research* 26, 779–798.
- Lakshmi, R.S., Satya Prakash, Lotliker, A.A., Baliarsingh, S.K., Samanta, A., Mathew, T., Chatterjee, A., Sahu B.K., Nair, T.M.B., 2021. Physicochemical controls on the initiation of phytoplankton bloom during the winter monsoon in the Arabian Sea. *Scientific Reports* 11:13448.

- Landry, M.R., Brown, S.L., Campbell, L., Constantinou, J., Liu, H., 1998. Spatial patterns in phytoplankton growth and microzooplankton grazing in the Arabian Sea during monsoon forcing. *Deep-Sea Research II* 45, 2353-2368.
- Landry, M.R., Selph, K.E., Brown, S.L., Abbott, M.R., Measures, C.I., Vink, S., Allen, C.B., Calbet, A., Christensen, S., Nolla, H., 2002. Seasonal dynamics of phytoplankton in the Antarctic Polar Front region at 170° W. *Deep-Sea Research Part II: Topical Studies in Oceanography* 49, 1843-1865.
- Leblanc, K., Quéguiner, B., Diaz, F., Cornet, V., Michel-Rodriguez, M., Durrieu de Madron X., Bowler, C., Malviya, S., Thyssen, M., Grégori, G., Rembauville, M., 2018. Nanoplanktonic diatoms are globally overlooked but play a role in spring blooms and carbon export. *Nature communications* 9, 953.
- Lee, D.B., Song, H.Y., Park, C., Choi, K.H., 2012. Copepod feeding in a coastal area of active tidal mixing: diel and monthly variations of grazing impacts on phytoplankton biomass. *Marine Ecology* 33, 88-105.
- Lee, Z., Weidemann, A., Kindle, J., Arnone, R., Carder, K.L., Davis, C., 2007. Euphotic zone depth: Its derivation and implication to ocean-color remote sensing. *Journal of Geophysical Research: Oceans*, 112.
- Levy, M., Shankar, D., Andre J.M., Shenoi, S.S.C., Durand F., Montegut C.D.B., 2007. Basin-wide seasonal evolution of the Indian Ocean's phytoplankton blooms. *Journal of Geophysical Research* 12, C12.
- Lynch, M., Shapiro, J., 1981. Predation, enrichment, and phytoplankton community structure. *Limnology and Oceanography* 26, 86-102.
- Mackey, M.D., Mackey, D.J., Higgins, H.W., Wright, S.W., 1996. CHEMTAX-a program for estimating class abundances from chemical markers: application to HPLC measurements of phytoplankton. *Marine Ecology Progress Series* 144, 265-283.
- Madhu, N.V., Jyothibabu, R., Balachandran, K.K., 2010. Monsoon-induced changes in the size-fractionated phytoplankton biomass and production rate in the estuarine and coastal waters of the southwest coast of India. *Environmental Monitoring and Assessment* 166, 521–528.
- Madhu, N.V., Martin G.D., Haridevi, C.K., Nair, M., Balachandran, K.K., Ullas, N., 2017. Differential environmental responses of tropical phytoplankton community in the southwest coast of India. *Regional Studies in Marine Science* 16, 21-35.
- Madhuprathap, M., Haridas, P., Ramaiah, N., Achuthankutty, C.T., 1992. Zooplankton of the southwest coast of India: abundance, composition, temporal and spatial variability in 1987. In: *Oceanography of Indian Ocean* (eds. Desai, B.N) Oxford & IBH, New Delhi, 99 – 112.
- Madhupratap, M., Kumar, S.P., Bhattathiri, P.M.A., Kumar, M.D., Raghukumar, S., Nair, K.K.C., Ramaiah, N., 1996. Mechanism of the biological response to winter cooling in the northeastern Arabian Sea. *Nature* 384, 549-552.
- Madhupratap, M., Nair, K.N.V., Gopalakrishnan, T.C., Haridas, P., Nair, K.K.C., Venugopal, P., Gauns, M., 2001. Arabian Sea oceanography and fisheries of the west coast of India. *Current Science* 81, 355-361.

- Malone, T.C., 1971. The relative importance of nanoplankton in and net-plankton as primary producers in tropical oceanic and neritic phytoplankton communities. *Limnology and Oceanography* 16, 633-639.
- Malone, T.C., 1980. Size-fractionated primary productivity of marine phytoplankton. In: *Primary productivity in the sea*. Springer, 301-319.
- Mann, K.H., 1993. Physical oceanography, food chains, and fish stocks: a review. *ICES Journal of Marine Science* 50, 105-119.
- Maranon, E., Steele, J., Thorpe, A., Turekian, K., 2009. Phytoplankton size structure. *Elements of physical oceanography: A derivative of the encyclopaedia of ocean sciences*, 85.
- Matondkar, S.G.P., Dwivedi, R.M., Parab, S., Pednekar, S., Mascarenhas, A., Raman, M., Singh, S., 2007. Phytoplankton in the Northeastern Arabian Sea exhibit seasonality. *SPIE Newsroom*. The International Society for Optical Engineering, pp. 2-4.
- McCarthy, J.J., Garside, C., Nevins, J.L., 1999. Nitrogen dynamics during the Arabian Sea northeast monsoon. *Deep-Sea Research Part II: Topical Studies in Oceanography* 46(8-9), 1623-1664.
- McCreary Jr, J.P., Yu, Z., Hood, R.R., Vinayachandran, P.N., Furue, R., Ishida, A., Richards, K.J., 2013. Dynamics of the Indian Ocean oxygen minimum zones. *Progress in Oceanography* 112, 15-37.
- McQueen, D.J., Johannes, M.R.S., Post, J.R., Stewart, T.J., Lean, D.R.S., 1989. Bottom-up and top-down impacts on freshwater pelagic community structure. *Ecological Monographs* 59, 289-309.
- Menon, N.N., Sankar, S., Smitha, A., George, G., Shalin, S., Sathyendranath, S., Platt, T., 2019. Satellite chlorophyll concentration as an aid to understanding the dynamics of Indian oil sardine in the southeastern Arabian Sea. *Marine Ecology Progress Series* 617-618: 137-147. doi.org/10.3354/meps12806.
- Metaxas, A., Scheibling R.E., 1996. Top-down and bottom-up regulation of phytoplankton assemblages in tidepools. *Marine Ecology Progress Series* 145, 161-177.
- MLR Plankton Atlas, 2011. Atlas on environmental parameters and productivity of the Indian EEZ and adjoining seas. Nair, K.K.C. (Ed.), Centre for Marine Living Resources and Ecology, Ministry of Earth Sciences, New Delhi, pp. 294.
- Mohan, A.P., Jyothibabu, R., Jagadeesan, L., Lallu, K.R., Karnan, C., 2016. Summer monsoon onset-induced changes of autotrophic pico- and nanoplankton in the largest monsoonal estuary along the west coast of India. *Environmental Monitoring and Assessment* 188, 93.
- Moreira-Turcq, P.F., Martin, J.M., 1998. Characterisation of fine particles by flow cytometry in estuarine and coastal Arctic waters. *Journal of Sea Research* 39, 217-226.
- Moreno, A.R., Martiny, A.C., 2018. Ecological Stoichiometry of Ocean Plankton. *Annual Review of Marine Science* 10, 43-69.
- Nair, P.G., Joseph, S., Kripa, V., Remya, R., Pillai, V.N., 2016. Growth and maturity of Indian oil sardine *Sardinella longiceps* (Valenciennes, 1847) along the southwest coast of India. *Journal of the Marine Biological Association of India* 58(1), 64-68.

- Nair, R.V., Subrahmanyam, R., 1955. The diatom, *Fragilaria oceanica* Cleve, an indicator of abundance of the Indian oil sardine, *Sardinella longiceps* Cuv. and Val. *Current Science* 24, 41-42.
- Nair, S.R.S., Devassy, V.P., Madhupratap, M., 1992. Blooms of phytoplankton along the west coast of India associated with nutrient enrichment and the response of zooplankton. *Science of the Total Environment* 819-828.
- Naqvi, S.W.A., 1987. Some aspects of the oxygen-deficient conditions and denitrification in the Arabian Sea. *Journal of Marine Research* 45,1049-1072.
- Naqvi, S.W.A., Noronha, R.J., Reddy, C.V.G., 1982. Denitrification in the Arabian Sea. *Deep-Sea Research Part A. Oceanographic Research Papers* 29, 459-469.
- Naqvi, S.W.A., Sarma, V., Jayakumar, D.A., 2002. Carbon cycling in the northern Arabian Sea during the northeast monsoon: Significance of salps. *Marine Ecology Progress Series* 226, 35-44.
- Paffenhofer, G.A., Strickler, J. R., Alcaraz, M., 1982. Suspension feeding by herbivorous calanoid copepods: A cinematographic study. *Marine Biology* 67, 193-199.
- Platt, T., Fuentes-Yaco, C., Frank, K.T., 2003. Spring algal bloom and larval fish survival. *Nature* 423, 398-399.
- Pomeroy, L.R., 1974. The ocean's food web, a changing paradigm. *Bioscience* 24, 499-504.
- Pomeroy, L.R., 2000. Food web connections: links and sinks. *Microbial biosystems: New frontiers. Atlantic Canada Society for Microbial Ecology*, 81-87.
- Prakash, P., Prakash, S., Rahaman, H., Ravichandran, M., Nayak, S., 2012. Is the trend in chlorophyll-a in the Arabian Sea decreasing? *Geophysical Research Letters*, p. 39, 10.1029/2012GL054187.
- Prasanna Kumar, S., Ramaiah, N., Gauns, M., Sarma, V., Muraleedharan, P.M., Raghukumar, S., Kumar, M.D., Madhupratap, M., 2001. Physical forcing of biological productivity in the Northern Arabian Sea during the Northeast Monsoon. *Deep-Sea Research Part II: Topical Studies in Oceanography* 48,1115-1126.
- Prasanna Kumar, S., Ramesh, R., Dwivedi, R.M., Raman, M., Sheshshayee, M.S., D'Souza, W., 2010. Nitrogen uptake in the northeastern Arabian Sea during winter cooling. *International Journal of Oceanography*, 819029.
- Price, H.J., Paffenhofer, G.A., Strickler J.R., 1983. Modes of cell capture in calanoid copepods. *Limnology and Oceanography* 28, 116-123.
- Qasim, S.Z., 2003. Endless Supply of Freshwater from Seawater Using Desalination Technologies. *Indian Journal of Public Administration* 49(3), 296-300.
- Quigg, A., Finkel, Z.V., Irwin, A. J., Rosenthal, Y., Ho, T.Y., Reinfelder, J.R., Schofield, O., Morel, F.M., Falkowski, P.G., 2003. The evolutionary inheritance of elemental stoichiometry in marine phytoplankton. *Nature* 425, 291–294.
- Quinlan, E.L., Jett, C.H., Philips, E.J., 2009. Microzooplankton grazing and the control of phytoplankton biomass in the Suwannee River estuary, USA. *Hydrobiologia* 632,127-137.

- Rao, C. A.V., Kurian, S., Vidya, P.J., Gauns, M., Shenoy, D.M., Mulla, A., Naik, H., Reddy, T.V., Naqvi, S.W.A., 2018. Phytoplankton response to the contrasting physical regimes in the eastern Arabian Sea during the northeast monsoon. *Journal of Marine Systems* 182, 56-66.
- Ramamirtham, C.P., Jayaraman, R., 1960. Hydrographical features of the continental shelf waters off Cochin during the years 1958 and 1959. *Journal of the Marine Biological Association of India* 2,199-207.
- Ramasastry, A.A., Myrland, P., 1959. Distribution of temperature, salinity and density in the Arabian Sea along the South Malabar Coast (South India) during the post-monsoon season. *Indian Journal of Fisheries* 6, 223-255.
- Redfield, A.C., Ketchum, B.H., Richards, F.A., 1963. The influence of organisms on the composition of seawater. *The sea* 2, 26-77.
- Ribeiro, C., Marie, D., Marie, D., Santos, A.L.D, Vaultot, D., 2016. Estimating microbial populations by flow cytometry: Comparison between instruments. *Limnology and Oceanography, Methods* 14(11).
- Robin, R.S., Kanuri, V.V., Muduli, P.R., Mishra, R.K., Jaikumar, M., Karthikeyan, P., Suresh Kumar, C., Saravana Kumar, C., 2013. Dinoflagellate bloom of *Karenia mikimotoi* along the southeast Arabian Sea, bordering western India. *Journal of Ecosystems* 2013.
- Rodriguez, E.G., Valentine, J.L., Andre, D.L., Jacob, S.A., 1992. Upwelling and downwelling at Cabo Frio (Brazil). Comparison of biomass and production responses. *Journal of Plankton Research* 14 (2), 289–306.
- Roesler, C., Uitz, J., Claustre, H., Boss, E., Xing, X., Organelli, E., Briggs, N., Bricaud. A., Schmechtig, C., Poteau, A., d'Ortenzio, F., 2017. Recommendations for obtaining unbiased chlorophyll estimates from in situ chlorophyll fluorometers: A global analysis of WET Labs ECO sensors. *Limnology and Oceanography, Methods* 15, 2017, 572–585.
- Roy, R., Anil, A.C., 2015. Complex interplay of physical forcing and Prochlorococcus population in the ocean. *Progress in Oceanography* 137, 250-260.
- Rykaczewski, R.R., Checkley, D.M., 2008. Influence of ocean winds on the pelagic ecosystem in upwelling regions. *Proceedings of the National Academy of Sciences* 105(6), 1965-1970.
- Ryther, J.H., 1969. Photosynthesis and fish production in the sea. *Science* 166(3901), 72-76.
- Santhikrishnan, S., Jyothibabu, R., Albin, K.J., Alok, K.T., Karnan, C., Arunpandi, N., Camey, M.F., Kumar, T.R.G., 2021. Biophysical implications of the freshwater influx over small spatial scale in the coastal waters along the southwest coast of India during the Southwest Monsoon. *Continental Shelf Research* 214,104337.
- Sarma, V., Bhaskar, T.V.S.U., Kumar, J.P., Chakraborty, K., 2020. Potential mechanisms responsible for occurrence of core oxygen minimum zone in the north-eastern Arabian Sea. *Deep-Sea Research Part I: Oceanographic Research Papers* 165,103393.
- Sarma, V., Patil, J.S., Shankar, D., Anil, A.C., 2019. Shallow convective mixing promotes massive *Noctiluca scintillans* bloom in the northeastern Arabian Sea. *Marine pollution bulletin* 138, 428-436.

- Sarma, V., Rao, G.D., Viswanadham, R., Sherin, C.K., Salisbury, J., Omand, M.M., Mahedevan, A., Murty, V.S.N., Shroyer, EL., Baumgartner, M., 2016. Effects of freshwater stratification on nutrients, dissolved oxygen and phytoplankton in the Bay of Bengal. *Oceanography* 29, 222-231.
- Sautour, B., Artigas, L.F., Delmas, D., Herbland, A., Laborde, P., 2000. Grazing impact of micro- and mesozooplankton during a spring situation in coastal waters off the Gironde estuary. *Journal of Plankton Research* 22, 531-552.
- Sawant, S.S., Madhupratap, M., 1996. Seasonality and composition of phytoplankton in the Arabian Sea. *Current Science* 71, 869-873.
- Schmidt, H., Czeschel, R., Visbeck, M., 2019. Ventilation dynamics of the Oxygen Minimum Zone in the Arabian Sea. *Biogeosciences Discussions* 1-32.
- Shafeeque, M., Shah, P., Platt, T., Sathyendranath, S., Menon, N.N., Balchand, A.N., and George, G., 2019. Effect of precipitation on Chlorophyll-a in an upwelling-dominated region along the west coast of India. *Journal of Coastal Research* 86, 218-224.
- Shalin, S., Sanilkumar, K.V., 2014. Variability of chlorophyll-a off the southwest coast of India. *International Journal of Remote Sensing* 35(14), 5420-5433.
- Shankar, D., Remya, R., Anil, A.C., Vijith., V., 2019. Role of physical processes in determining the nature of fisheries in the eastern Arabian Sea. *Progress in Oceanography* 172, 124-158.
- Shenoy, D.M., Suresh, I., Uskaikar, H., Kurian, S., Vidya, P.J., Shirodkar, G., Gauns, M.U., Naqvi, S.W.A., 2020. Variability of dissolved oxygen in the Arabian Sea Oxygen Minimum Zone and its driving mechanisms. *Journal of Marine Systems* 204,103310.
- Sherman, K., Smith, W., Morse, W., Berman, M., Green, J., Ejsymont, L., 1984. Spawning strategies of fishes in relation to circulation, phytoplankton production, and pulses in zooplankton off the northeastern United States. *Marine ecology progress series*. Oldendorf 18,1-19.
- Shetye, S.R., Gouveia, A.D., Shenoi, S.S.C., Sundar, D., Michael, G.S., Almeida, A.M., Santanam, K., 1990. Hydrography and circulation off the west coast of India during the southwest monsoon 1987. *Journal of Marine Research* 48, 359-378.
- Shetye, S.R., Suresh, I., Shankar, D., Sundar, D., Jayakumar, S., Mehra, P., Prabhudesai, R.G. Pednekar, P.S., 2008. Observational evidence for remote forcing of the West India Coastal Current. *Journal of Geophysical Research: Oceans* 113 (C11).
- Shi, W., Wang, M., 2022. Phytoplankton biomass dynamics in the Arabian Sea from VIIRS observations. *Journal of Marine Systems* 227, 103670, doi.org/10.1016/j.jmarsys.2021.103670.
- Sieburth, J.M., Smetacek, V., Lenz, Jr., 1978. Pelagic ecosystem structure: Heterotrophic compartments of the plankton and their relationship to plankton size fractions 1. *Limnology and oceanography* 23, 1256-1263.
- Smitha, B.R., Sanjeevan, V.N., Vimalkumar, K.G., Revichandran, C., 2008. On the upwelling off the southern tip and along the west coast of India. *Journal of Coastal Research* 95-102.

- Subrahmanian, R., 1959. Studies on the phytoplankton of the west coast of India. *Proceedings of the Indian Academy of Sciences* 50, 189-252.
- Tackx, M.L.M., Bakker, C., Francke, J.W., Vink M., 1989. Size and phytoplankton selection by Oosterschelde zooplankton. *Netherlands Journal of Sea Research* 23, 35-43.
- Threlkeld, S.T., 1988. Planktivory and planktivore biomass effects on zooplankton, phytoplankton, and the trophic cascade *Limnology and Oceanography* 33, 1362-1375.
- Tilstone, G.H., Figueiras, F.G., Fermin, E.G., Arbones, B., 1999. Significance of nanophytoplankton photosynthesis and primary production in a coastal upwelling system (Ria de Vigo, NW Spain). *Marine Ecology Progress Series* 183, 13-27.
- Tseng, Y.F., Lin, J., Dai, M., Kao, S.J., 2014. Joint effect of freshwater plume and coastal upwelling on phytoplankton growth off the Changjiang River. *Biogeosciences* 11, 409-423.
- UNESCO., 1994. *Protocols for the Joint Global Ocean Flux Study (JGOFS). Core Measurements.* UNESCO, Paris 29, pp. 170.
- Vanni, M., 1987. Effects of nutrients and zooplankton size on the structure of a phytoplankton community. *Ecology* 68, 624-635.
- Vanni, M., Findlay, D.L., 1990. Trophic cascades and phytoplankton community structure. *Ecology* 71, 921-937.
- Vanni, M., Temte, J., 1990. Seasonal patterns of grazing and nutrient limitation of phytoplankton in a eutrophic lake. *Limnology and Oceanography* 35, 699-709.
- Vaulot, D., LeBot, N., Marie, D., Fukai, E., 1996. Effect of phosphorus on the *Synechococcus* cell cycle in surface Mediterranean waters during summer. *Applied and Environmental Microbiology* 62, 2527-2533.
- Vijayan, A.K., Reddy, B.B., Sudheesh, V., Marathe, P.H., Nampoothiri, V.N., Harikrishnachari, N.V., Kavya, P., Gupta, G.V.M., Ramanamurthy, M.V., 2021. Phytoplankton community structure in a contrasting physicochemical regime along the eastern Arabian Sea during the winter monsoon. *Journal of Marine Systems* 215, 103501.
- Vijith, V., Vinayachandran, P.N., Thushara, V., Amol, P., Shankar, D., Anil, AC., 2016. Consequences of inhibition of mixed layer deepening by the West India Coastal Current for winter phytoplankton bloom in the northeastern Arabian Sea. *Journal of Geophysical Research: Oceans* 121, 6583-6603.
- Wassman, P., 1991. Dynamics of primary production and sedimentation in shallow fjords and pols of western Norway. *Oceanography and Marine Biology an Annual Review* 29, 87-154.

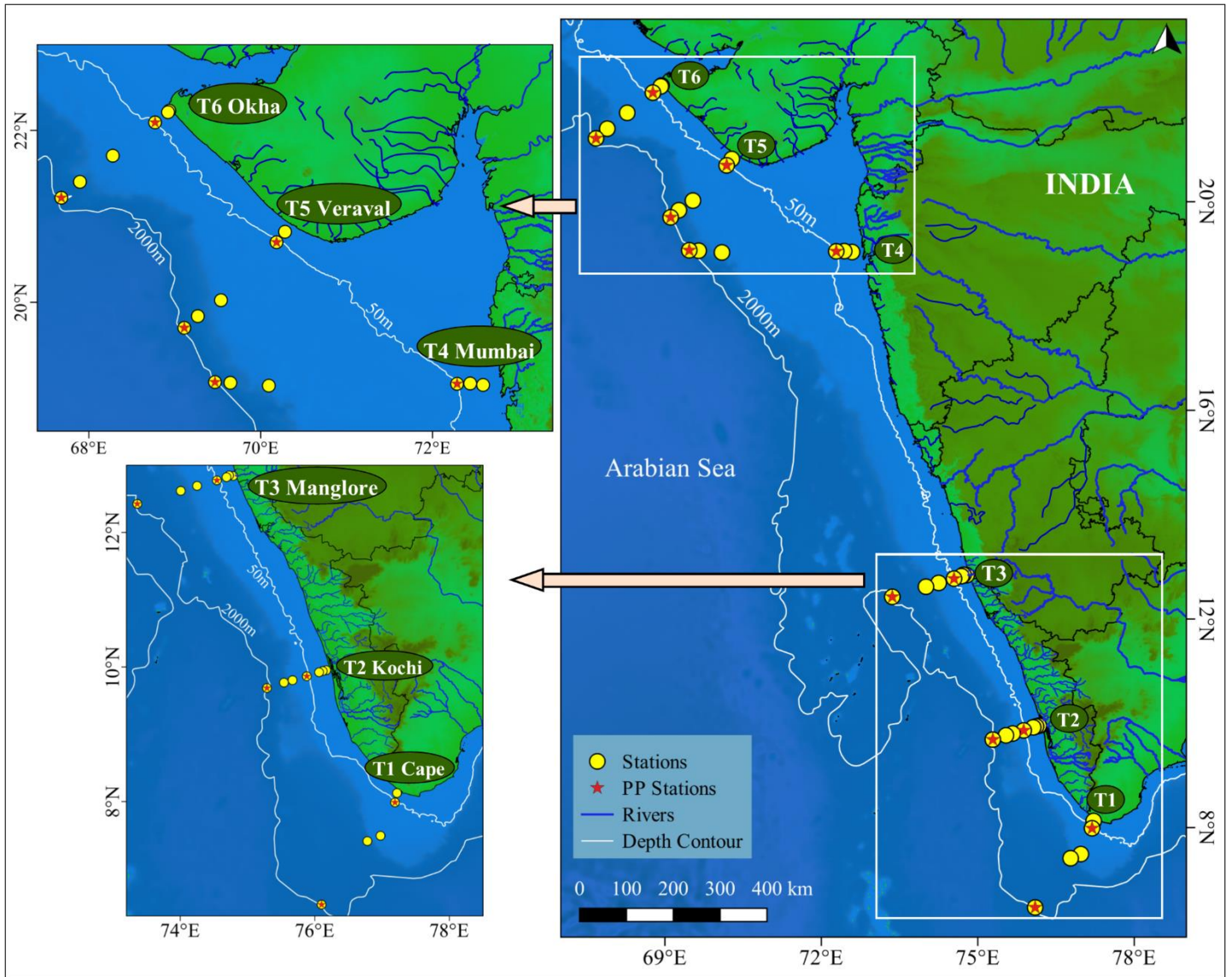


Figure 1 - Study area in the EAS and sampling locations. Cross-shore transects T1, T2, and T3 represents the SEAS whereas transects T4, T5 and T6 the NEAS. The depth of stations in each transect varies from 10 m to 2000 m and 6 to eight locations were sampled from each transect. Primary productivity locations are labelled with star marks. Some of the shallow locations were not sampled following the safety (rocky coast) of the ship.

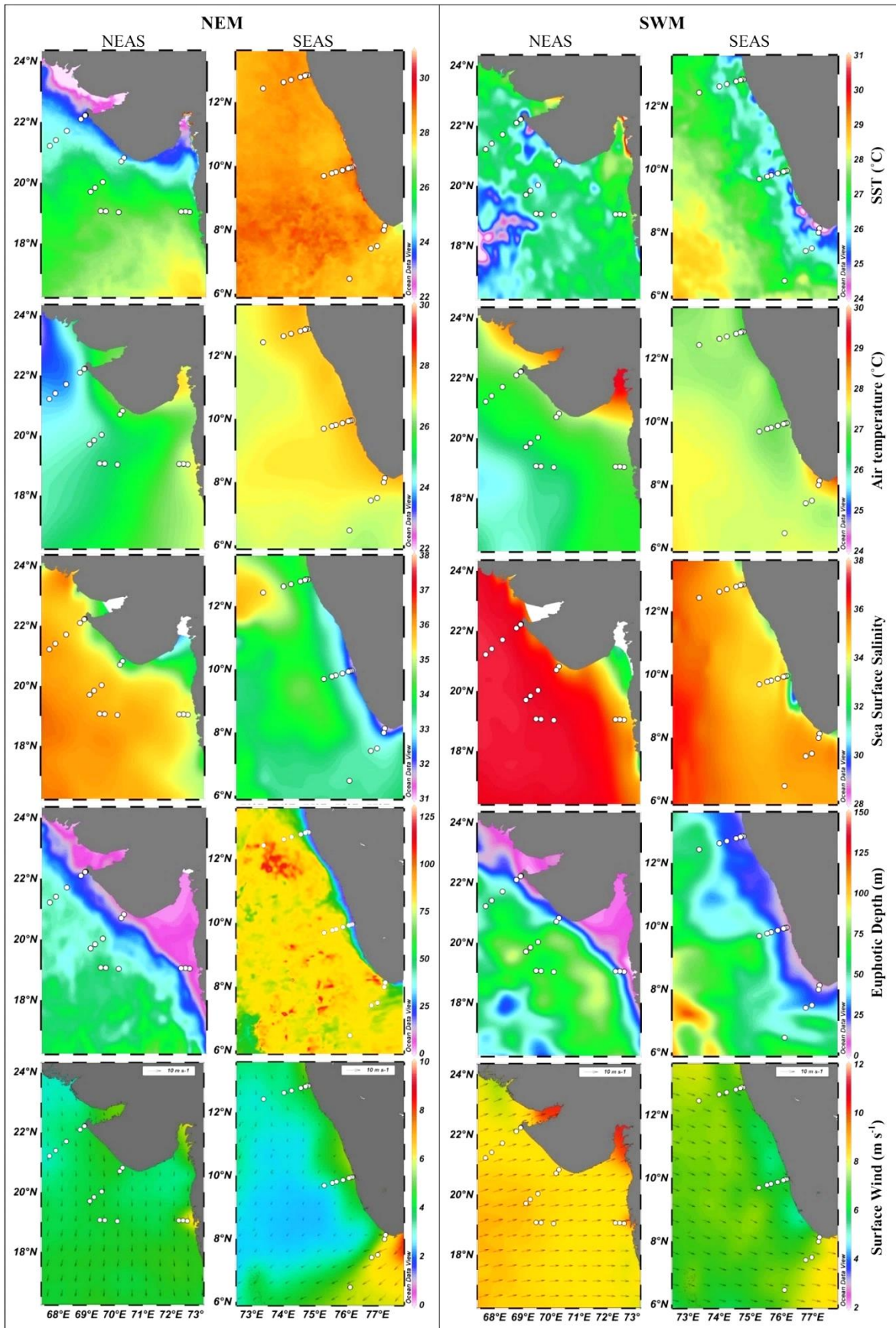


Figure 2 - Distribution of meteorological and ocean physical variables [Sea surface temperature (SST - °C), Air temperature (°C), Sea surface salinity (SSS), Euphotic depth (m), wind (m s^{-1})]. NEM - Northeast Monsoon, SWM - Southwest Monsoon, SEAS - Southeastern Arabian Sea and NEAS - Northeastern Arabian Sea

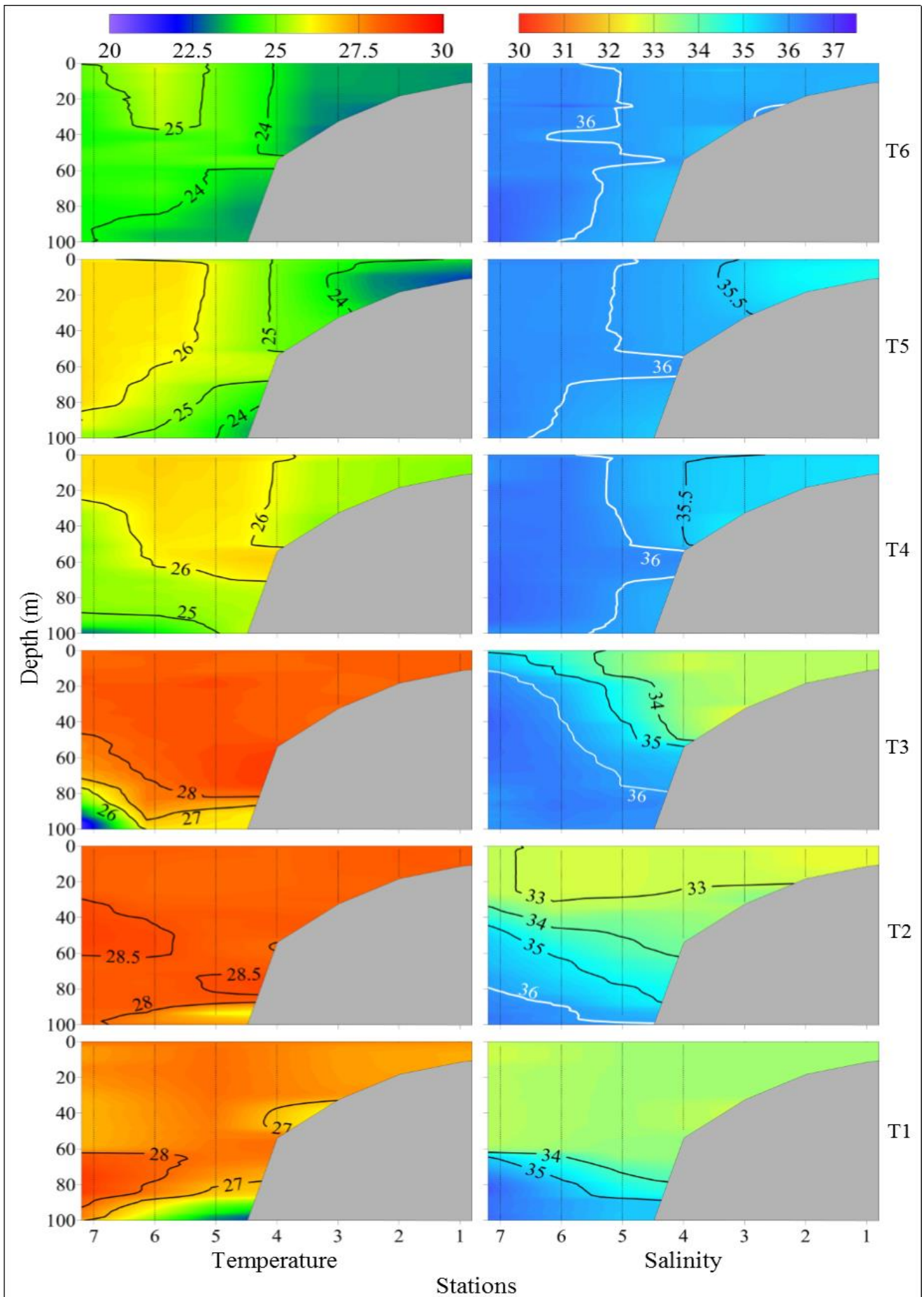


Figure 3 - Vertical distribution of temperature (°C) and salinity along various transects in the EAS during the NEM.

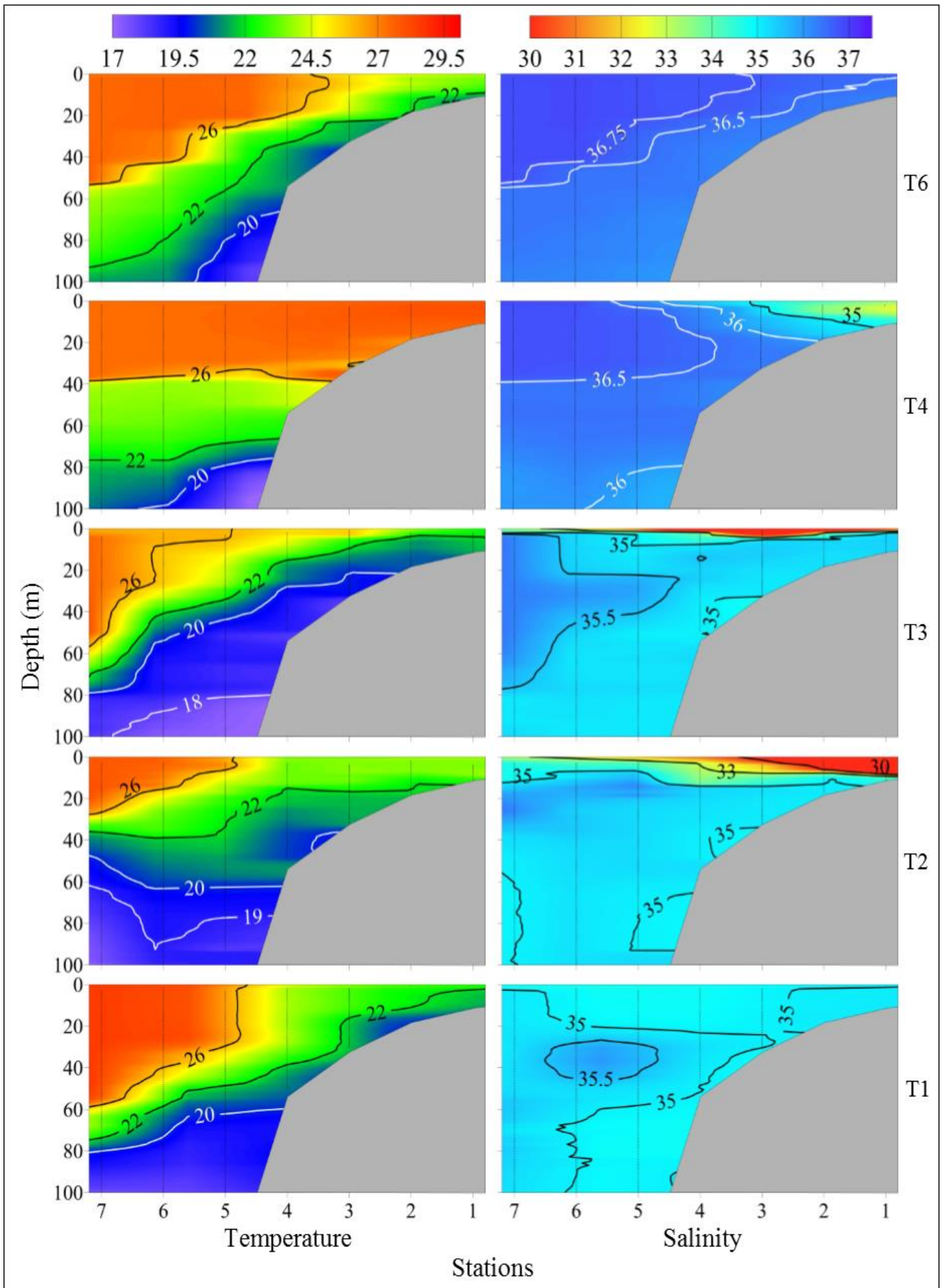


Figure 4 - Vertical distribution of temperature (°C) and salinity along various transects in the EAS during the SWM.

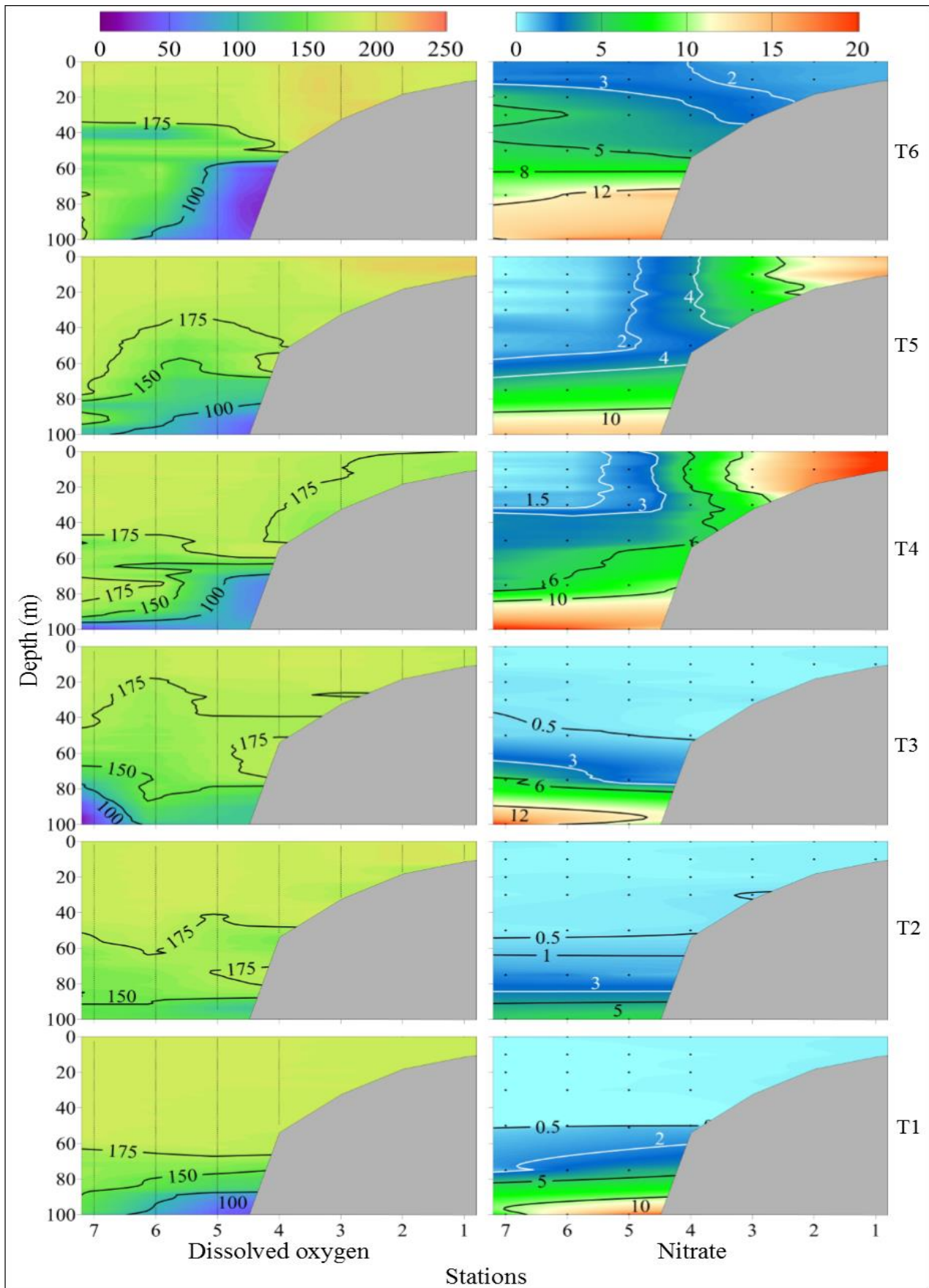


Figure 5 - Vertical distribution of dissolved oxygen (μM) and nitrate (μM) along various transects in the EAS during the NEM.

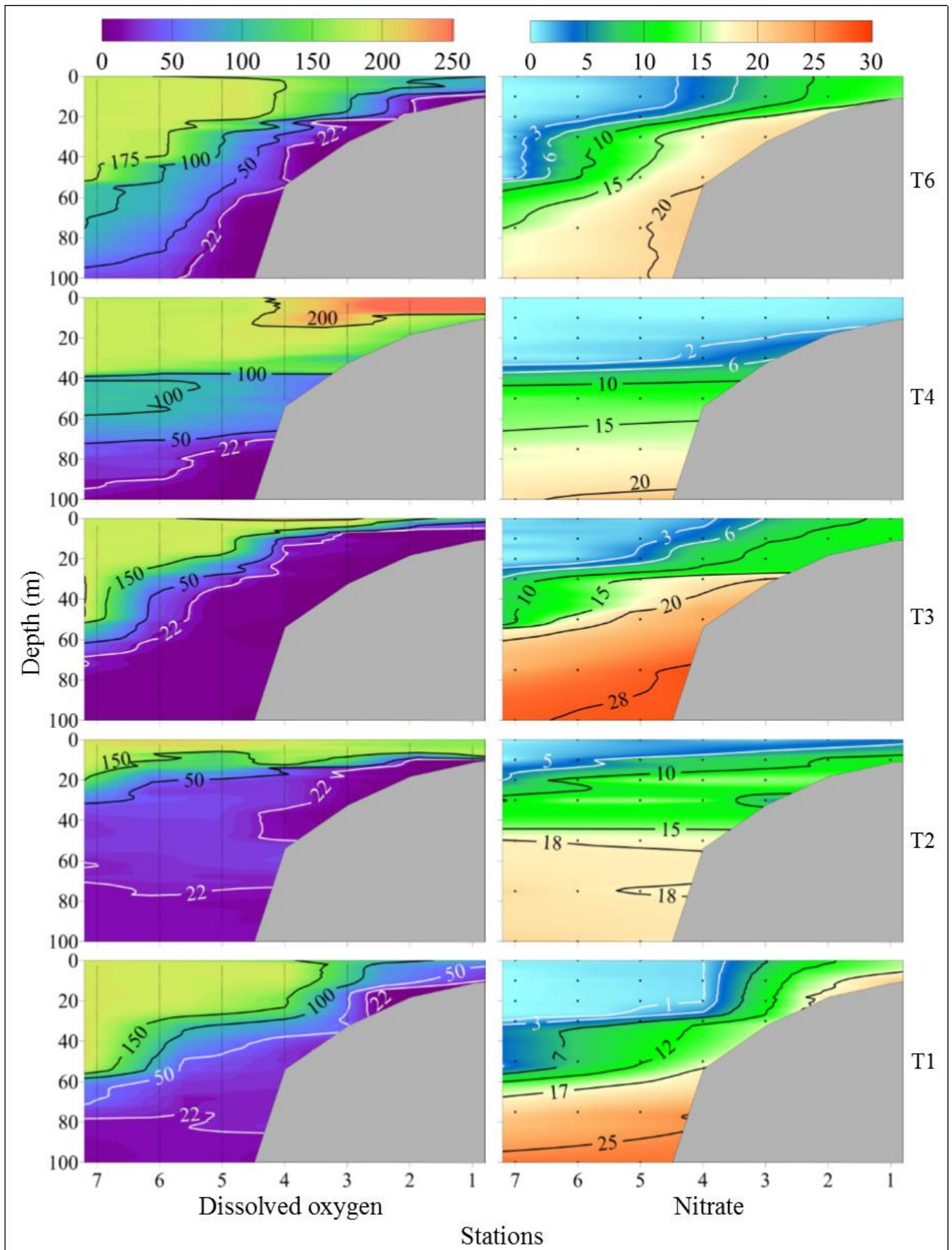


Figure 6 - Vertical distribution of dissolved oxygen (μM) and nitrate (μM) along various transects in the EAS during the SWM.

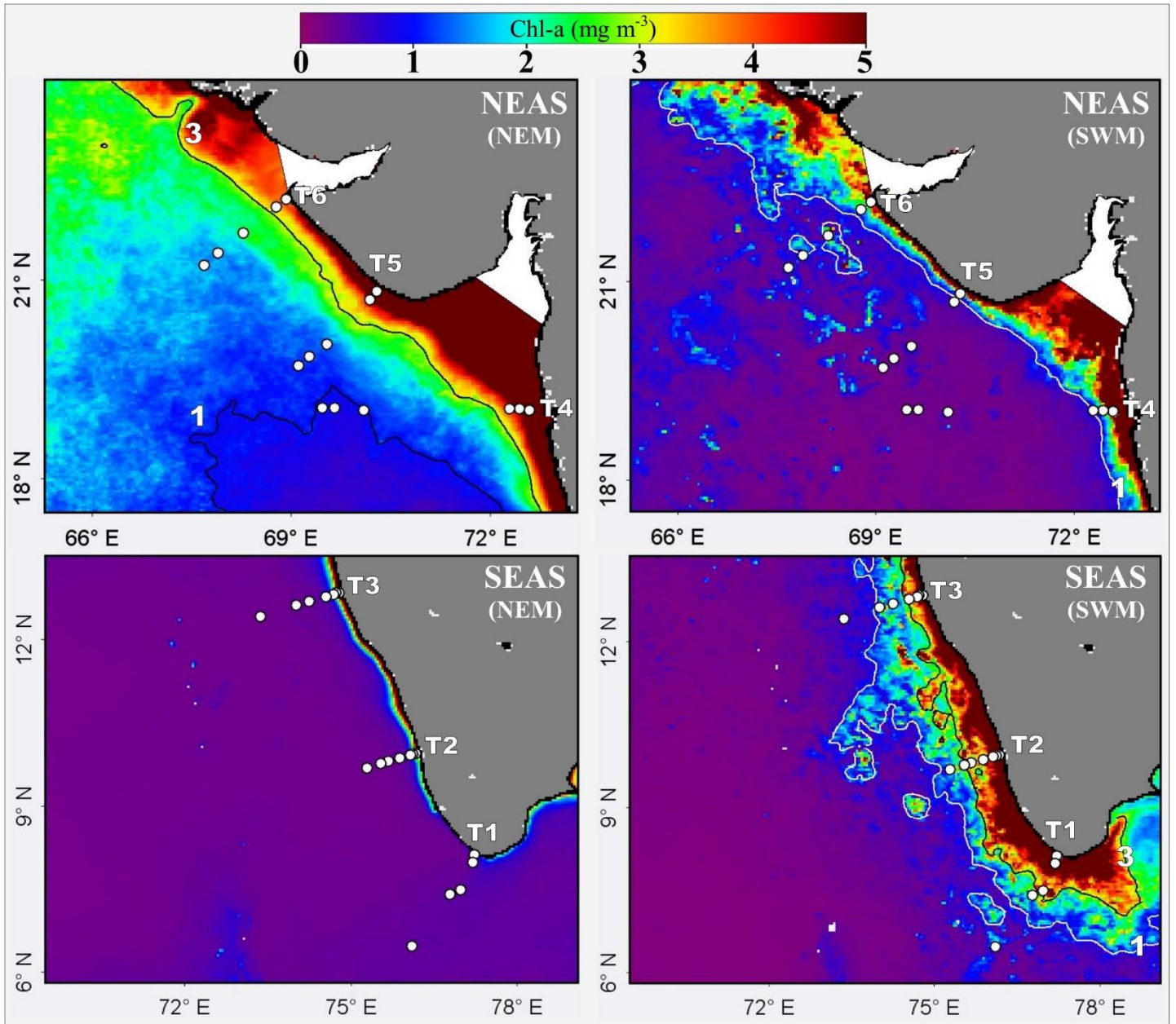


Figure 7 - Synoptic distribution pattern of phytoplankton biomass (Chl-a) in the EAS during different seasons reflected in the ocean colour data.

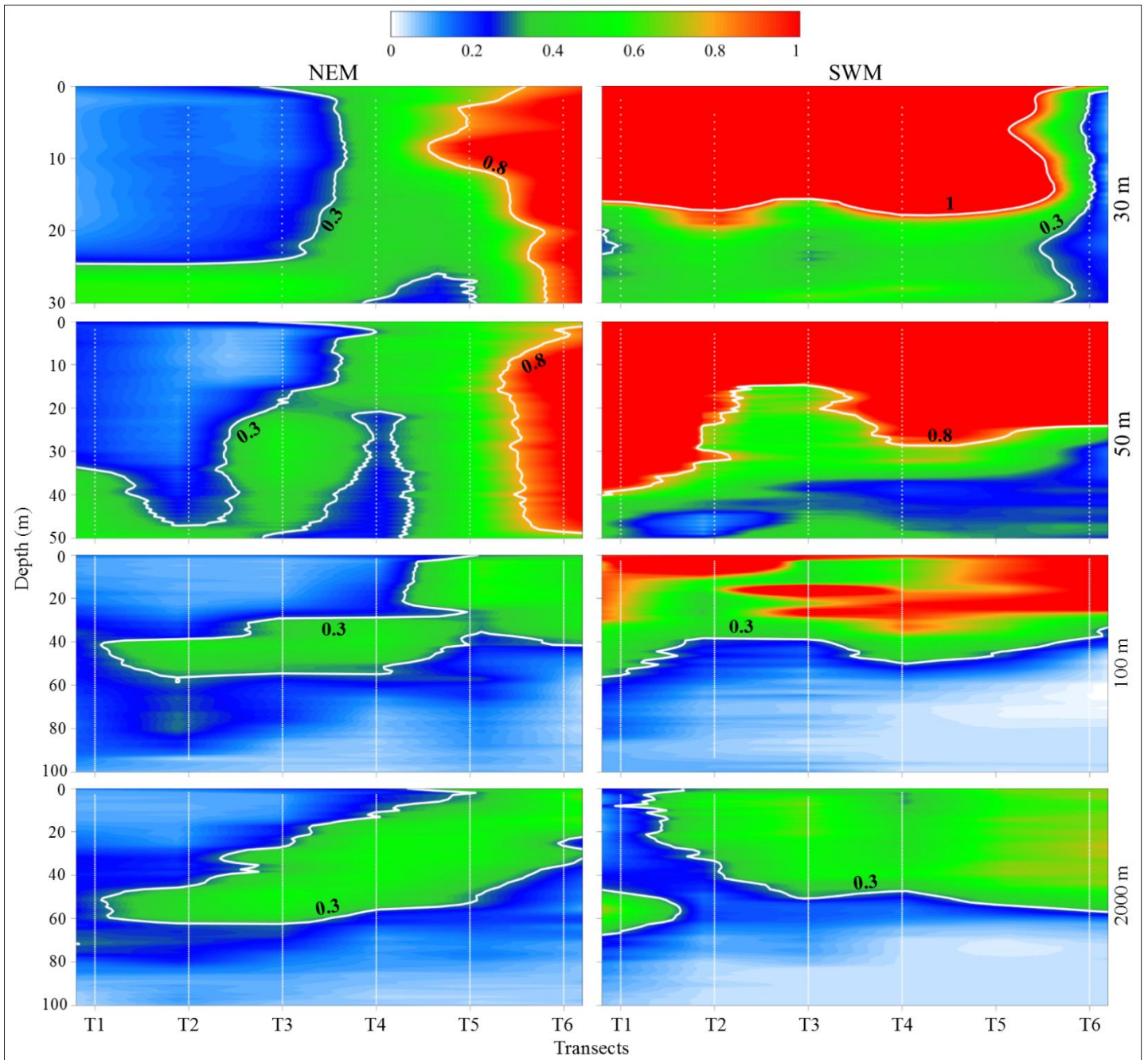


Figure 8 - The spatial and seasonal variations in the vertical distribution of phytoplankton biomass [Chl-a (mg m^{-3})] maxima layer along different depth contours (30m, 50m, 100m and 2000m) in the Indian western shelf and slope waters. It clearly shows the disappearance of subsurface chlorophyll maximum (SCM) and its northward shallowing during the NEM. Almost a complete absence of SCM was evident during SWM along the entire basin.

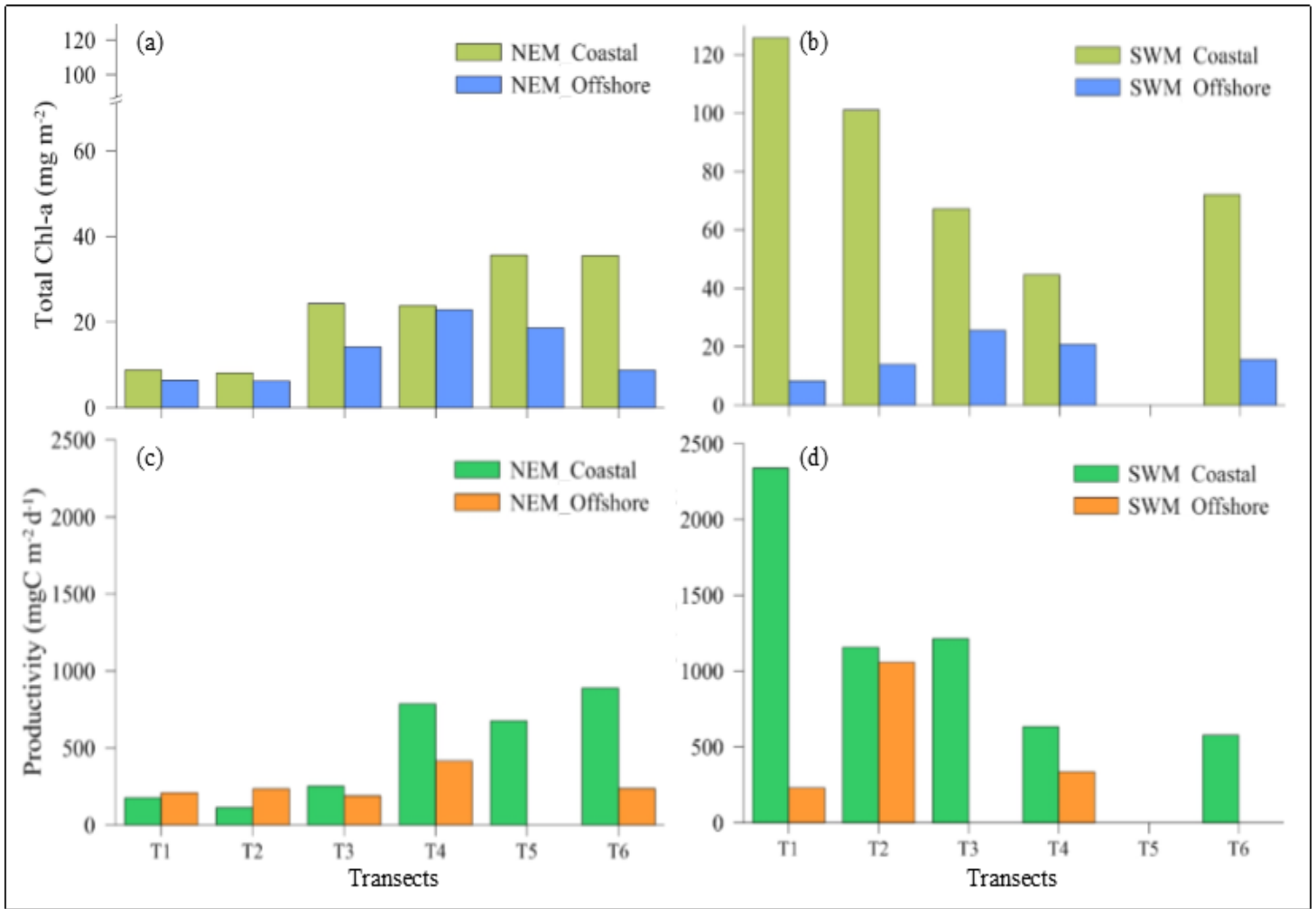


Figure 9 - Spatial and seasonal variations in phytoplankton biomass (Chl-a) [(a) NEM (b) SWM] and primary production [(c) NEM and (d) SWM] in the EAS. The discrete depth values of Chl-a and primary production for upper 50m are integrated and presented here as column values.

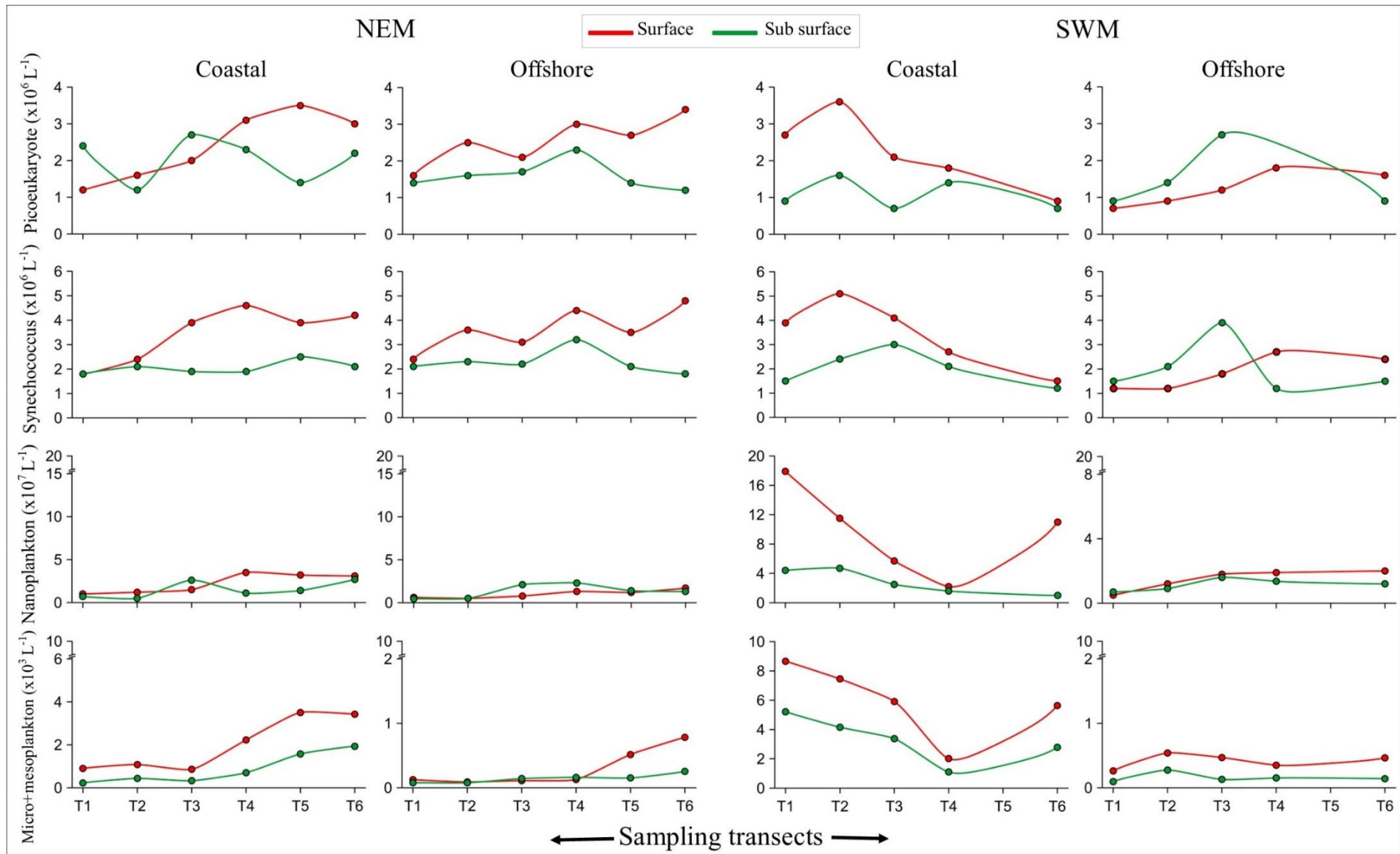


Figure 10 - The spatial and seasonal variations in the abundance of different phytoplankton size classes in the EAS. Surface and subsurface (30m) data in primary productivity locations in the coastal and offshore regions are shown.

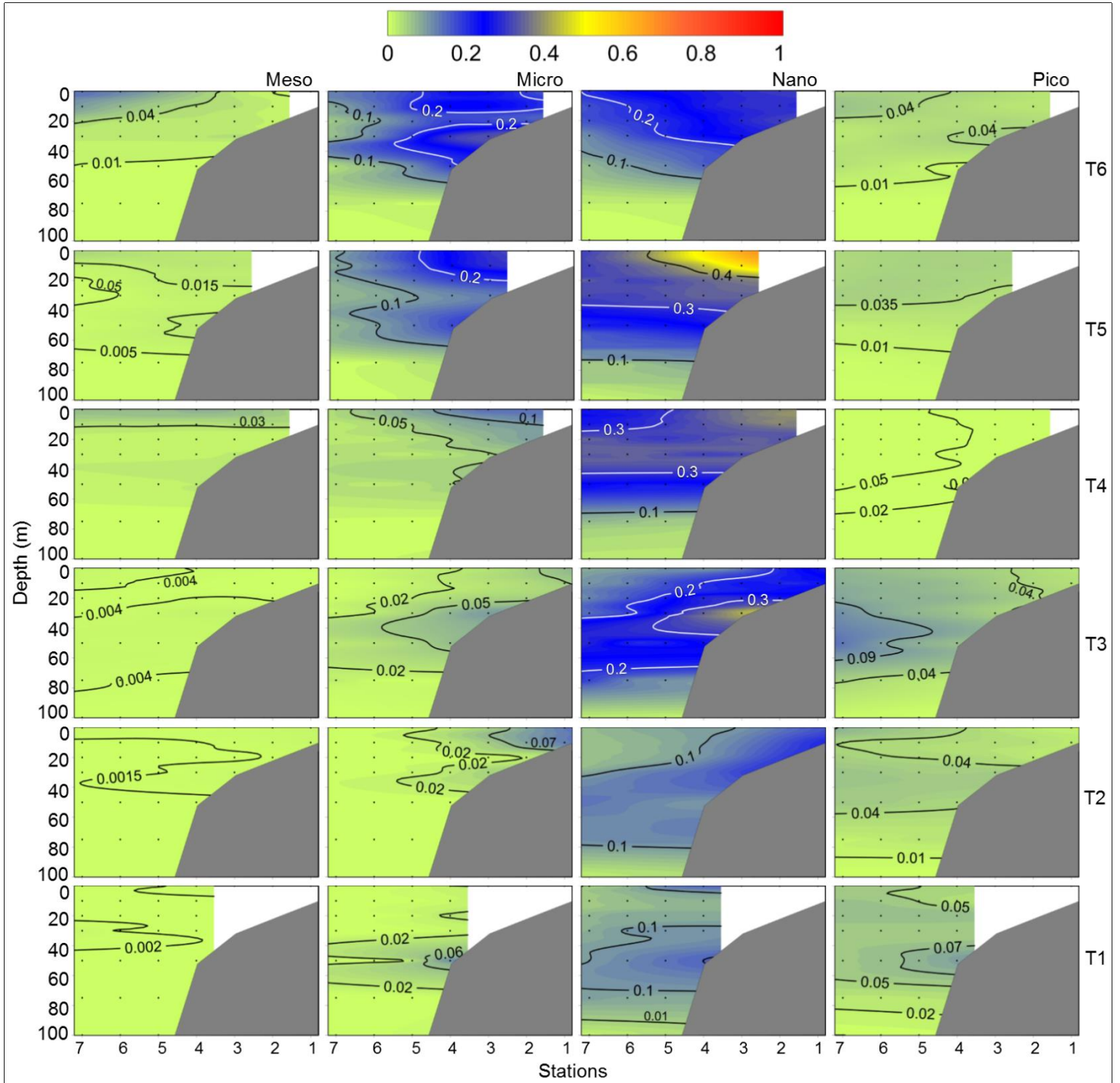


Figure 11 - The spatial variations in the vertical distribution of different phytoplankton size classes contribution to total Chl-a (mg m⁻³) during NEM. White colour represents no data.

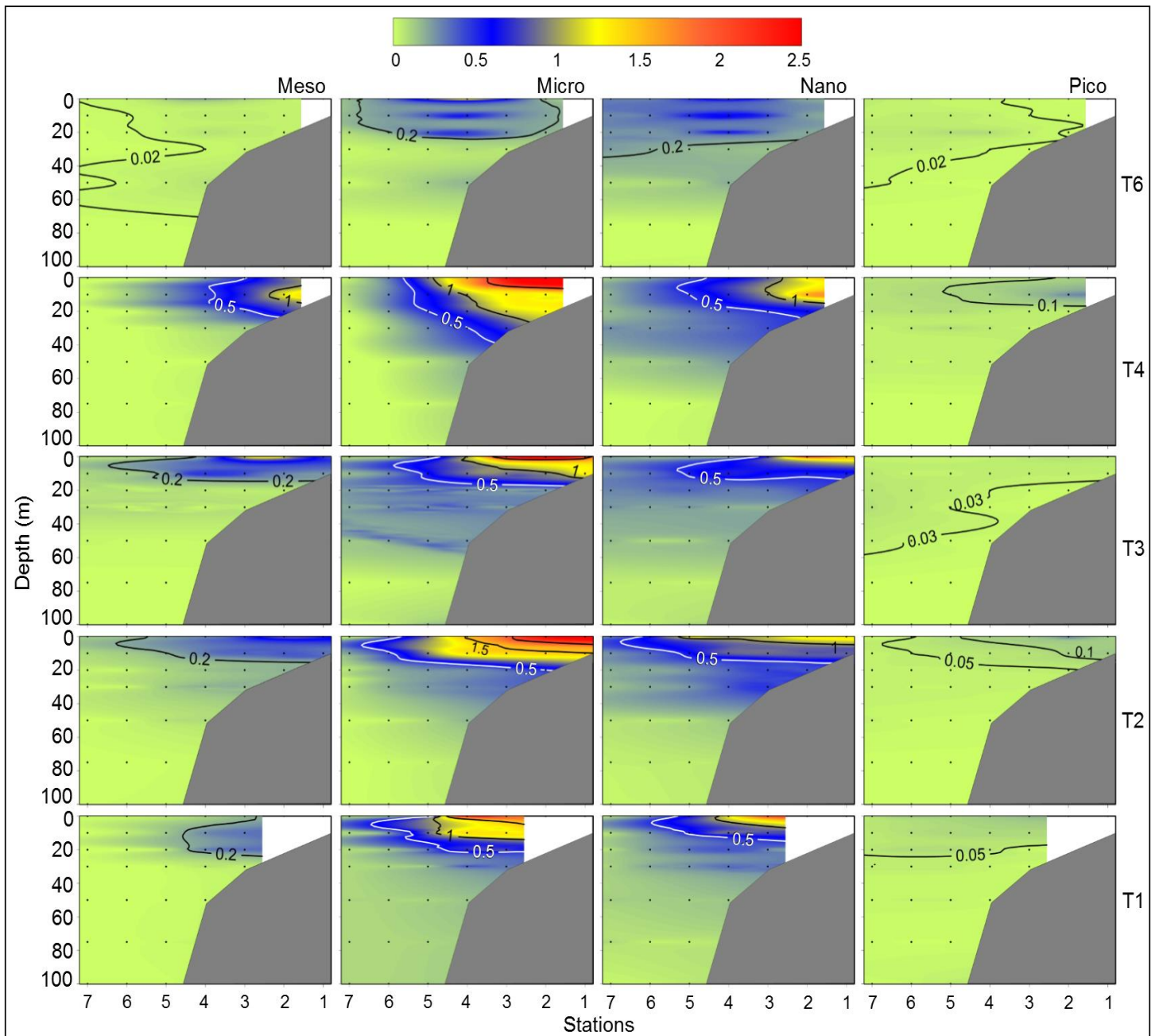


Figure 12 - The spatial variations in the vertical distribution of different phytoplankton size classes contribution to total Chl-a (mg m^{-3}) during SWM. The white colour represents no data.

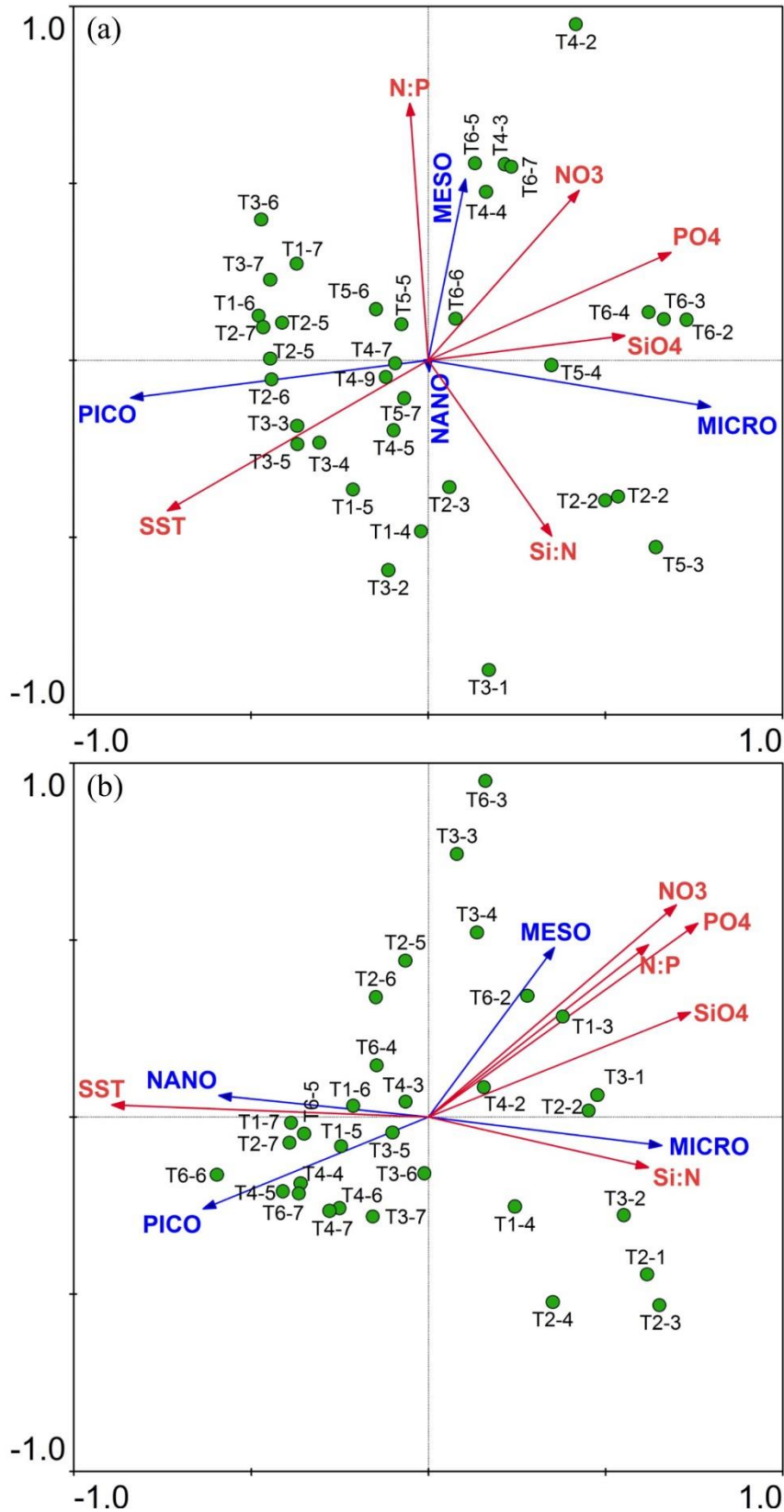


Figure 13 - RDA Triplot showing the interrelationship between physicochemical and biological variables during (a) NEM and (b) SWM. Red arrows and labels represent the physicochemical variables and the blue colour denotes phytoplankton size groups. Green dots represent the locations. MESO - mesoplankton, MICRO - microplankton, NANO - nanoplankton, PICO - picoplankton

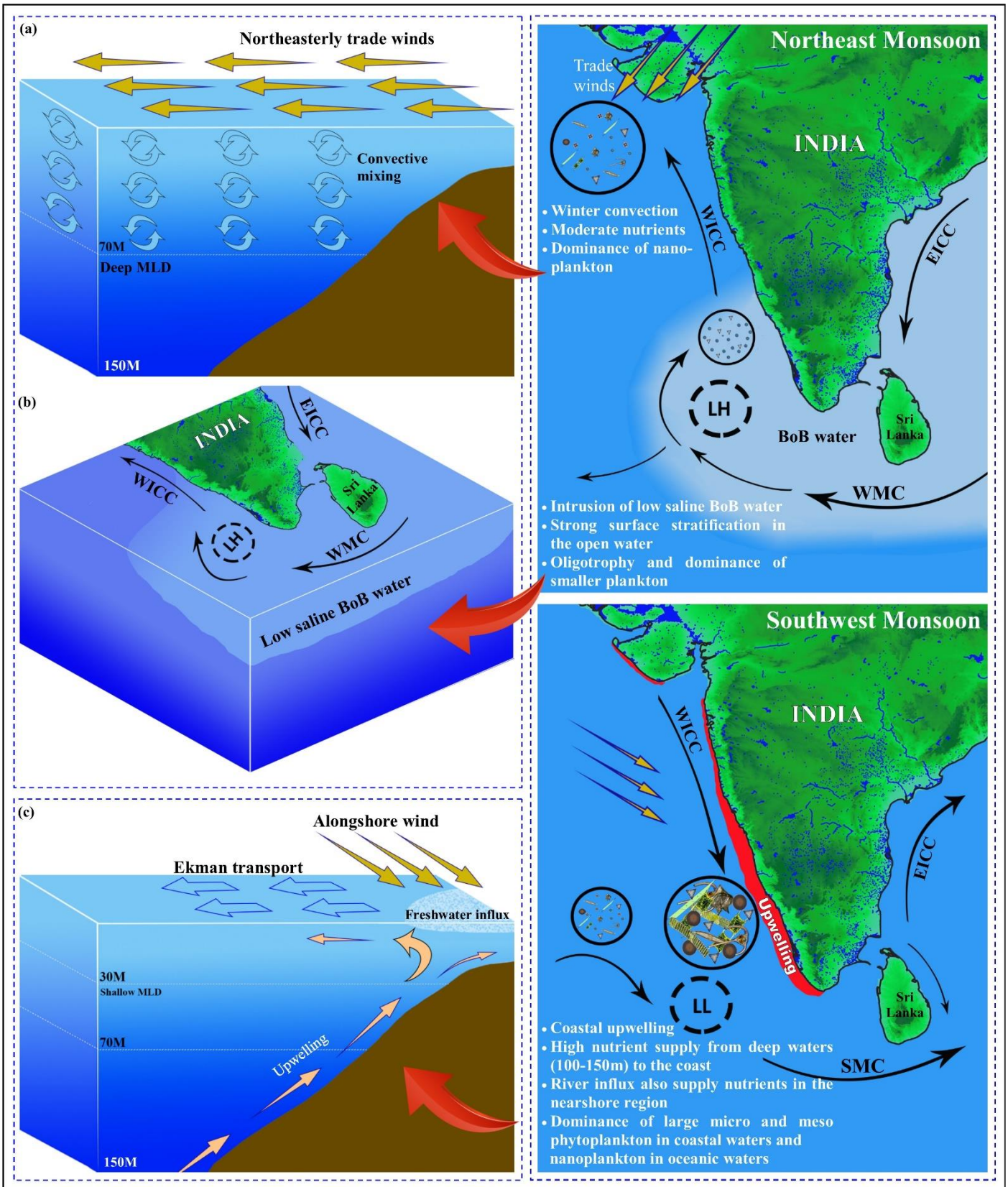


Figure 14 - Schematic interpretation of seasonal hydrographical setting and phytoplankton size response in the EAS during the NEM [(a) convective mixing prevails in the NEAS and (b) BoB water intrusion and stratification dominates in the SEAS] and the SWM [(c) coastal upwelling prevails in the NEAS and SEAS, more prominently in the latter]. During the NEM, the upper euphotic column was moderately rich in nutrients in the NEAS while the SEAS experiences impoverished nutrient levels due to the surface stratification associated with the low saline BoB water intrusion leading to the increased contribution of the smaller phytoplankton size class. During the SWM, the surface water layer (10-30 m) has significantly high nutrient concentration in the shelf waters due to coastal upwelling causing a noticeable increase in the larger phytoplankton size classes.

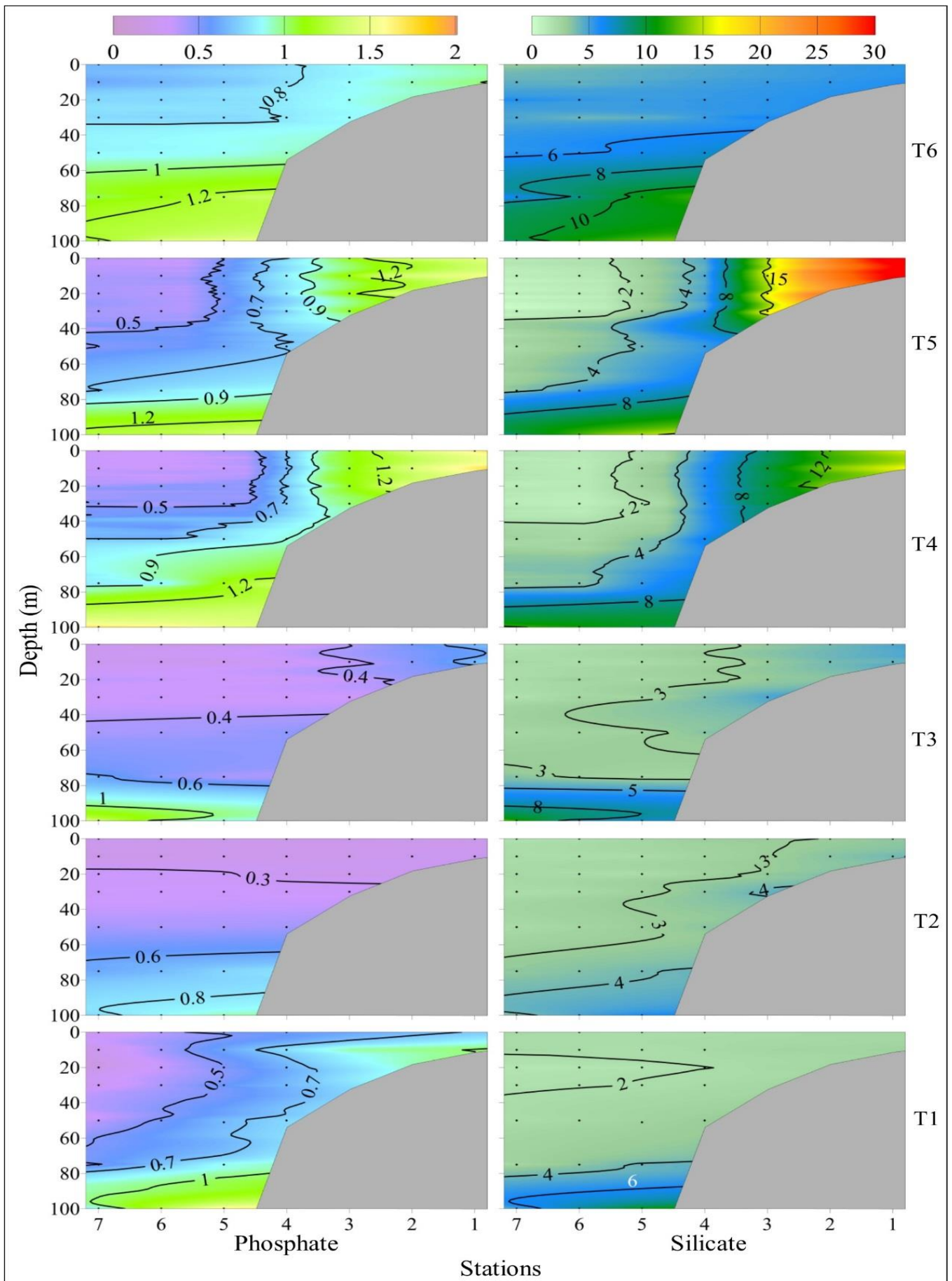
Parameters	SEAS		NEAS	
	Coastal	Offshore	Coastal	Offshore
Temperature (°C)	28.18 ± 0.26 (23 ± 1.07)	28.10 ± 0.27 (27.25 ± 0.95)	24.42 ± 0.99 (26.93 ± 1.63)	26.08 ± 0.73 (27.42 ± 0.08)
Salinity	32.96 ± 0.20 (31.49 ± 4.2)	33.45 ± 0.92 (34.93 ± 0.64)	35.52 ± 0.25 (35.88 ± 1.25)	36.12 ± 0.14 (36.82 ± 0.06)
MLD (m)	25.33 ± 12.12 (9.70 ± 6.97)	30.44 ± 17.08 (24.88 ± 6.57)	33.75 ± 13.83 (12 ± 5.76)	52.88 ± 23.75 (38 ± 9.38)
Euphotic column (m)	30.0 ± 16.58 (16.3 ± 6.41)	88.21 ± 5.47 (38.21 ± 7.84)	13.57 ± 3.98 (20.06 ± 8.11)	40.26 ± 4.66 (56.93 ± 5.43)
NO ₃ (µM)	0.21 ± 0.11 (11.02 ± 3.55)	0.19 ± 0.08 (4.33 ± 3.73)	5.04 ± 4.77 (2.77 ± 2.06)	0.62 ± 0.45 (0.11 ± 0.11)
SiO ₂ (µM)	3.43 ± 0.92 (18.34 ± 11.37)	1.99 ± 0.12 (3.38 ± 2.19)	10.49 ± 7.89 (8.22 ± 6.18)	3.01 ± 0.83 (0.91 ± 0.43)
PO ₄ (µM)	0.39 ± 0.20 (1.15 ± 0.21)	0.32 ± 0.12 (0.65 ± 0.25)	1.02 ± 0.30 (0.94 ± 0.50)	0.49 ± 0.13 (0.37 ± 0.09)
PP (mg C m ⁻² d ⁻¹)	181.1 ± 69.7 (1571.2 ± 665.8)	212.3 ± 23.3 (644.7 ± 586.4)	784.3 ± 106.1 (516.2 ± 158.2)	326.3 ± 126.2 (606.1 ± 39.5)
N:P	2.90 ± 1.87 (11.21 ± 2.6)	6.04 ± 1.91 (7.79 ± 3.52)	7.38 ± 4.42 (7.36 ± 2.89)	4.5 ± 1.75 (3.44 ± 2.32)
N:Si	0.32 ± 0.21 (0.91 ± 0.58)	0.92 ± 0.29 (1.57 ± 0.49)	0.77 ± 0.39 (1.01 ± 0.31)	0.73 ± 0.29 (1.43 ± 0.65)
Si:P	10.6 ± 4.13 (16.52 ± 11.76)	6.89 ± 1.85 (4.86 ± 1.8)	9.63 ± 5.05 (7.82 ± 3.28)	6.15 ± 0.75 (2.34 ± 0.59)
Surface waters				
Total Chl-a (mg m ⁻³)	0.22 ± 0.12 (3.80 ± 1.70)	0.17 ± 0.07 (0.64 ± 0.46)	0.70 ± 0.28 (1.10 ± 0.98)	0.38 ± 0.11 (0.48 ± 0.16)
Meso. Chl-a (mg m ⁻³)	- (0.22 ± 0.18)	- (0.05 ± 0.05)	0.03 ± 0.02 (0.02 ± 0.02)	0.03 ± 0.03 (0.01 ± 0.01)
Micro. Chl-a (mg m ⁻³)	0.07 ± 0.08 (2.20 ± 1.58)	- (0.06 ± 0.04)	0.30 ± 0.18 (0.93 ± 0.90)	0.05 ± 0.04 (0.03 ± 0.02)
Nano. Chl-a (mg m ⁻³)	0.13 ± 0.10 (1.24 ± 0.65)	0.08 ± 0.05 (0.29 ± 0.17)	0.45 ± 0.21 (0.48 ± 0.31)	0.25 ± 0.08 (0.26 ± 0.10)
Pico. Chl-a (mg m ⁻³)	0.03 ± 0.02 (0.12 ± 0.11)	0.06 ± 0.03 (0.05 ± 0.05)	0.04 ± 0.04 (0.05 ± 0.04)	0.04 ± 0.02 (0.05 ± 0.03)
Water column				
Total Chl-a (mg m ⁻²)	8.46 ± 6.57 (60.9 ± 35.36)	15.3 ± 6.11 (29.19 ± 10.86)	22.01 ± 10.55 (32.29 ± 26.44)	20.23 ± 6.08 (22.31 ± 2.84)
Meso. Chl-a (mg m ⁻²)	0.11 ± 0.16 (9.09 ± 3.97)	0.11 ± 0.21 (1.59 ± 1.35)	1.21 ± 0.78 (3.84 ± 3.07)	0.89 ± 1.07 (0.14 ± 0.14)
Micro. Chl-a (mg m ⁻²)	1.27 ± 1.02 (32.28 ± 19.94)	0.31 ± 0.3 (1.23 ± 0.71)	4.72 ± 3.34 (20.11 ± 18.24)	2.37 ± 1.23 (2.62 ± 2.25)
Nano. Chl-a (mg m ⁻²)	5.56 ± 4.43 (19.16 ± 8.94)	10.67 ± 3.76 (13.93 ± 3.55)	12.86 ± 4.68 (16.39 ± 11.27)	14.86 ± 5.38 (11.52 ± 2.5)
Pico. Chl-a (mg m ⁻²)	1.48 ± 1.34 (1.69 ± 1.18)	4.43 ± 2.31 (2.91 ± 1.77)	1.12 ± 0.62 (1.63 ± 1.43)	2.88 ± 1.47 (3.04 ± 1.07)

Table 1 - Spatial and seasonal variations in physicochemical and biological variables in the EAS during the NEM and the SWM. Nutrient concentrations are the mean values of the upper 30m water column. Data of SWM are presented in brackets. Hyphen indicate undetectable levels.

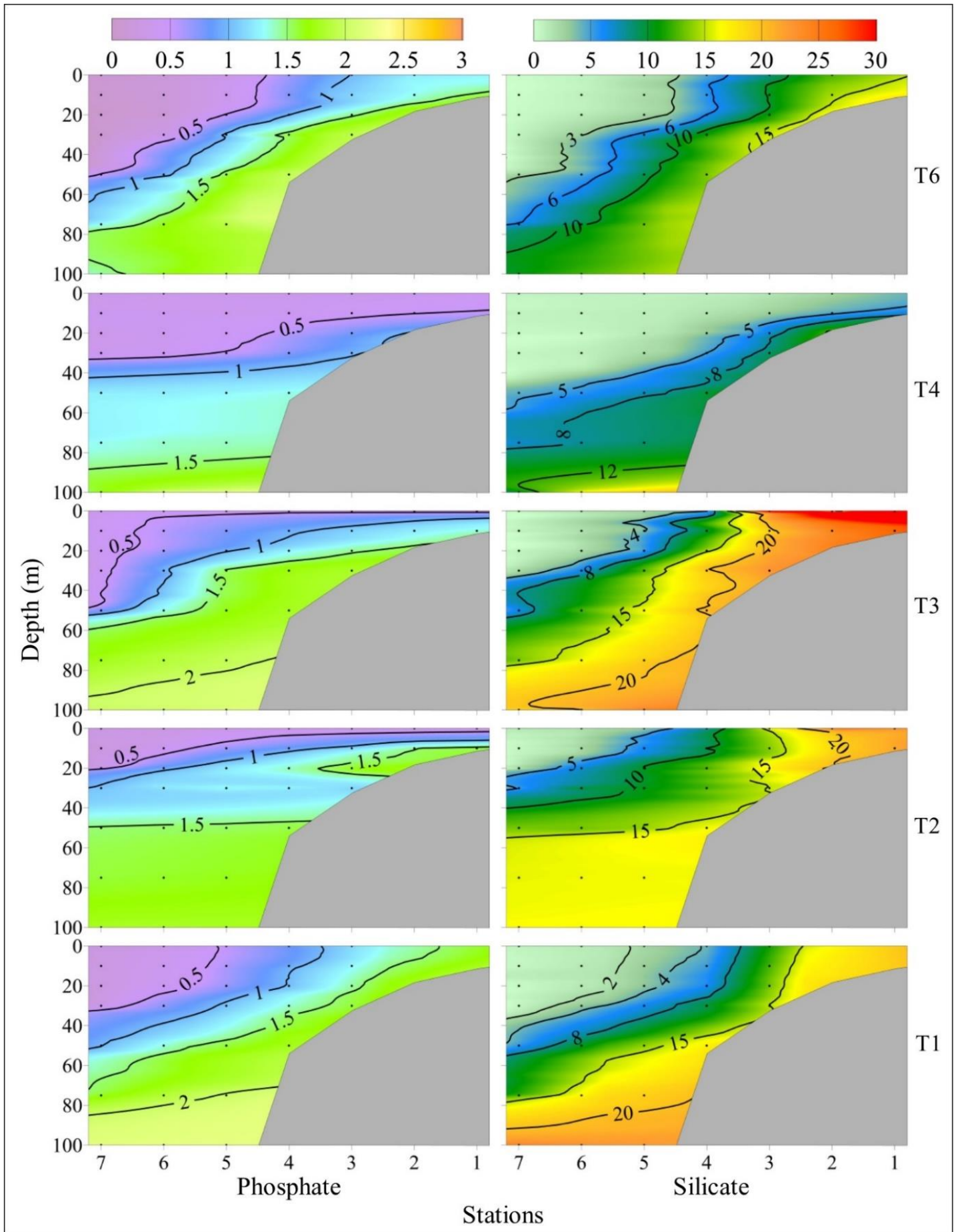
Genus	Coastal						Offshore					
	T1	T2	T3	T4	T5	T6	T1	T2	T3	T4	T5	T6
<i>Asterionella</i>	31 (15)	33 (94)	41 (84)	54 (88)	316 (NS)	532 (57)	2 (-)	- (7)	6 (-)	15 (-)	29 (NS)	33 (-)
<i>Ceratium</i>	33 (258)	51 (220)	11 (8)	9 (60)	124 (NS)	246 (125)	- (41)	5 (59)	13 (31)	8 (103)	56 (NS)	41 (42)
<i>Chaetoceros</i>	337 (154)	384 (206)	271 (269)	- (35)	647 (NS)	651 (38)	10 (32)	11 (97)	9 (57)	34 (59)	117 (NS)	206 (27)
<i>Coscinodiscus</i>	63 (957)	59 (1408)	33 (451)	24 (295)	211 (NS)	65 (346)	27 (81)	13 (74)	10 (88)	8 (40)	17 (NS)	40 (51)
<i>Dictyocha</i>	4 (46)	35 (18)	- (43)	- (26)	33 (NS)	32 (18)	1 (3)	- (11)	- (13)	- (-)	- (NS)	13 (4)
<i>Dinophysis</i>	7 (347)	3 (37)	5 (51)	12 (-)	22 (NS)	5 (30)	- (-)	- (11)	- (7)	- (7)	- (NS)	- (-)
<i>Fragilaria</i>	- (10)	- (54)	- (39)	- (-)	- (NS)	- (-)	- (-)	- (-)	- (-)	- (-)	- (NS)	- (-)
<i>Gymnodinium</i>	11 (43)	8 (37)	- (29)	74 (41)	101 (NS)	69 (20)	- (3)	- (9)	- (4)	18 (-)	33 (NS)	31 (2)
<i>Heliotheca</i>	- (-)	- (-)	- (-)	2 (-)	14 (NS)	28 (-)	- (-)	- (-)	- (-)	- (-)	5 (NS)	6 (-)
<i>Hemiaulus</i>	2 (48)	2 (-)	- (-)	22 (-)	40 (NS)	23 (11)	- (-)	- (-)	- (19)	21 (-)	6 (NS)	- (18)
<i>Hemidiscus</i>	3 (64)	- (27)	1 (18)	- (-)	- (NS)	9 (-)	- (-)	- (-)	- (-)	- (-)	- (NS)	5 (-)
<i>Navicula</i>	- (5)	11 (11)	- (29)	- (7)	- (NS)	- (7)	6 (-)	2 (7)	- (11)	- (-)	6 (NS)	- (3)
<i>Nitzschia</i>	45 (26)	- (91)	69 (-)	- (-)	- (NS)	87 (35)	33 (2)	16 (6)	6 (-)	4 (5)	33 (NS)	47 (5)
<i>Odontella</i>	81 (11)	66 (14)	37 (21)	24 (148)	51 (NS)	124 (34)	- (-)	- (8)	- (4)	- (2)	- (NS)	66 (-)
<i>Planktionella</i>	2 (20)	4 (9)	21 (-)	- (-)	53 (NS)	17 (5)	- (2)	- (17)	- (10)	- (4)	- (NS)	12 (-)
<i>Pleurosigma</i>	5 (34)	11 (17)	30 (39)	11 (18)	45 (NS)	62 (11)	3 (8)	9 (20)	7 (9)	- (-)	- (NS)	8 (-)
<i>Pseudo-nitzschia</i>	- (64)	9 (44)	- (107)	- (14)	- (NS)	- (20)	3 (12)	- (27)	- (-)	- (-)	- (NS)	5 (-)

<i>Rhizosolenia</i>	194 (5047)	245 (3361)	181 (2825)	98 (685)	354 (NS)	581 (4600)	7 (27)	4 (84)	- (128)	- (64)	78 (NS)	167 (242)
<i>Thalassionem a</i>	34 (354)	109 (542)	95 (822)	1940 (135)	130 (NS)	949 (71)	23 (38)	21 (56)	45 (51)	25 (29)	94 (NS)	78 (21)
<i>Thalassiosira</i>	36 (206)	31 (341)	38 (435)	34 (262)	241 (NS)	- (18)	11 (11)	9 (38)	5 (42)	8 (32)	68 (NS)	51 (26)
<i>Triceratium</i>	5 (26)	1 (30)	- (22)	- (22)	33 (NS)	- (7)	- (4)	- (7)	- (-)	2 (-)	- (NS)	- (14)
<i>Others</i>	20 (965)	28 (927)	31 (651)	- (220)	12 (NS)	17 (195)	- (-)	- (11)	9 (-)	3 (6)	7 (NS)	4 (11)

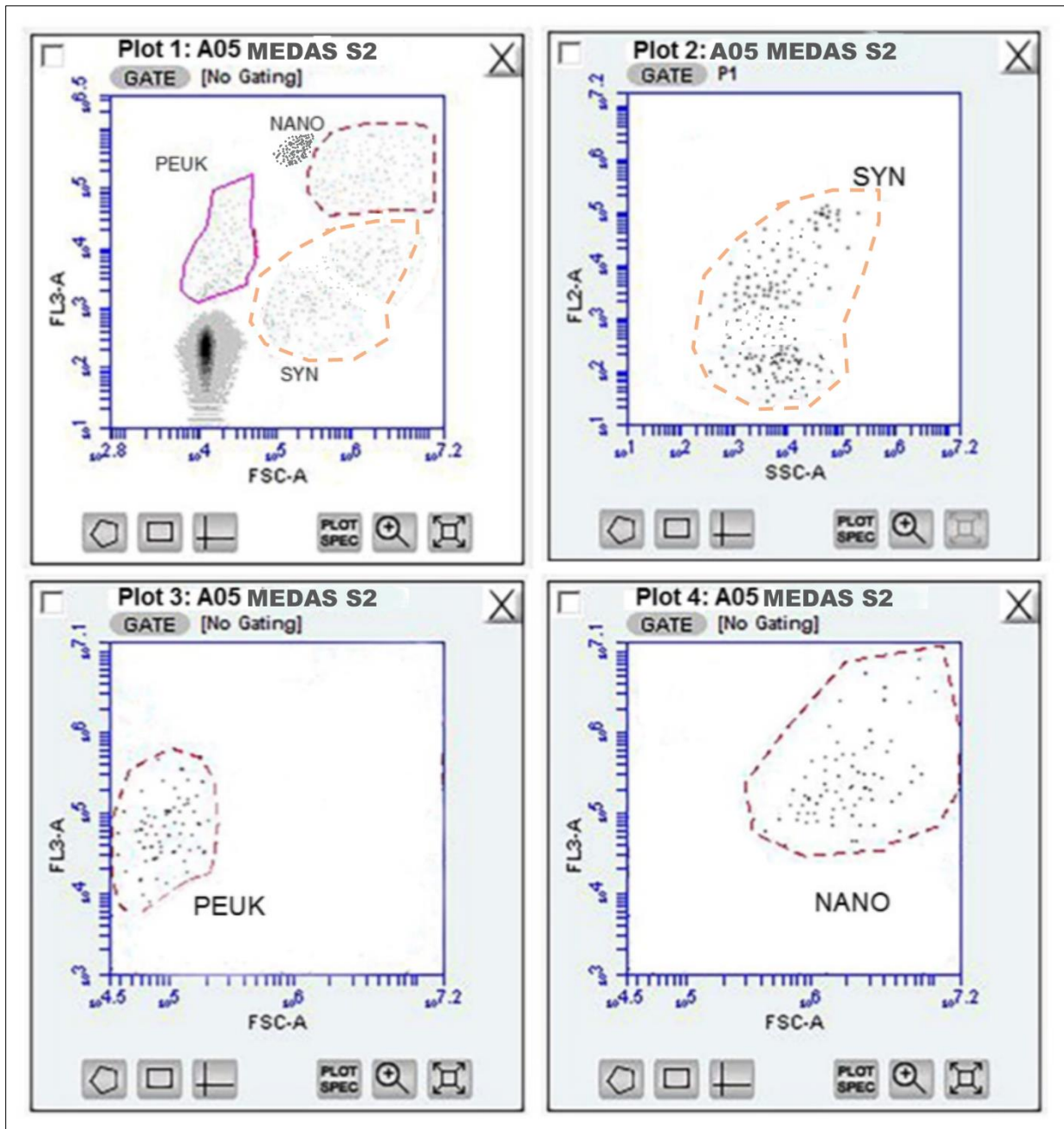
Table 2 – Micro-phytoplankton abundance of major genera (L^{-1}) during NEM and SWM (in brackets) from coastal (50m depth) and offshore (2000m) stations of EAS. NS - No sample, - absence.



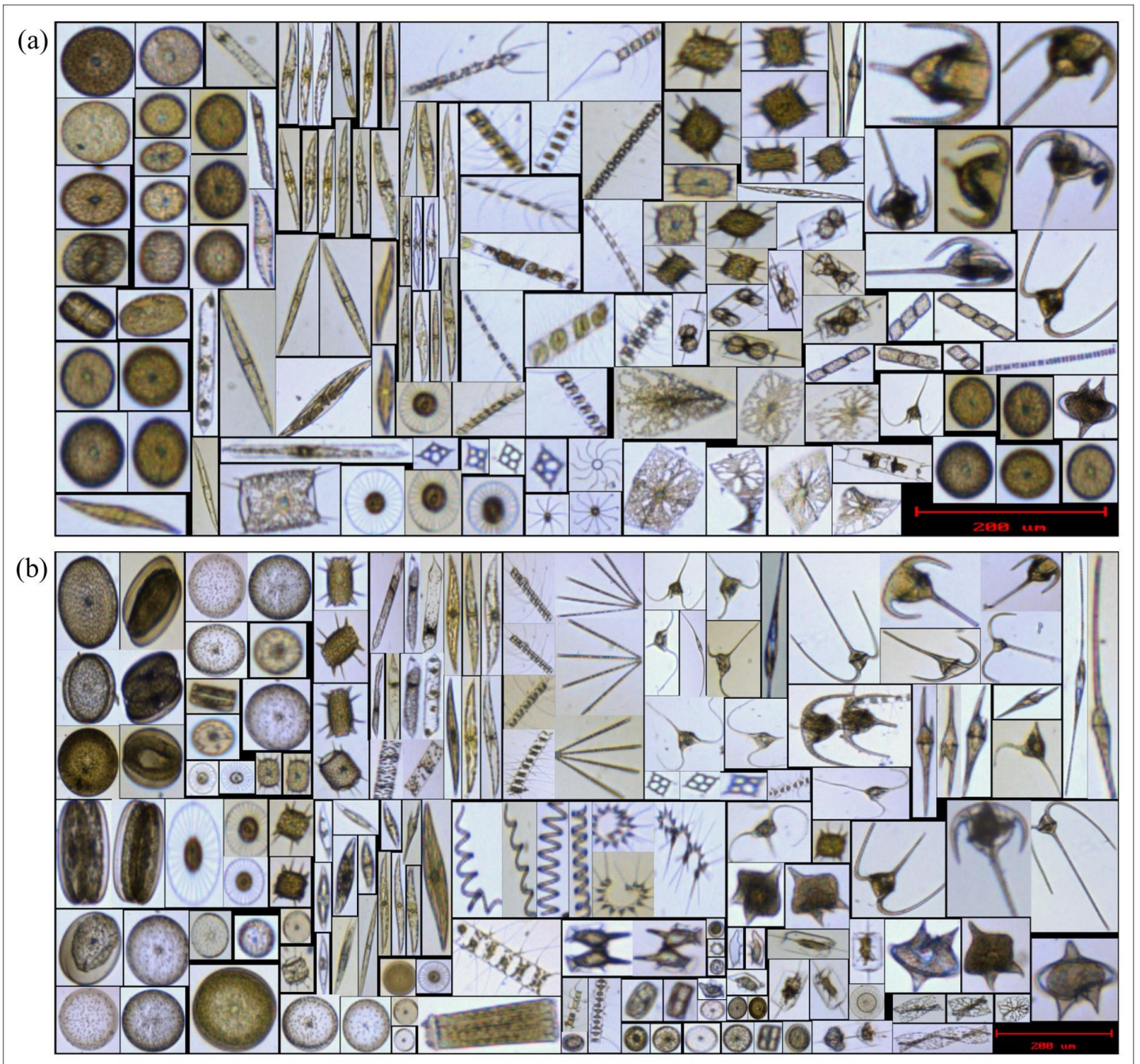
Supplementary Figure 1 - Vertical distribution of phosphate (mM) and silicate (mM) along various cross-shore transects in the EAS during the NEM.



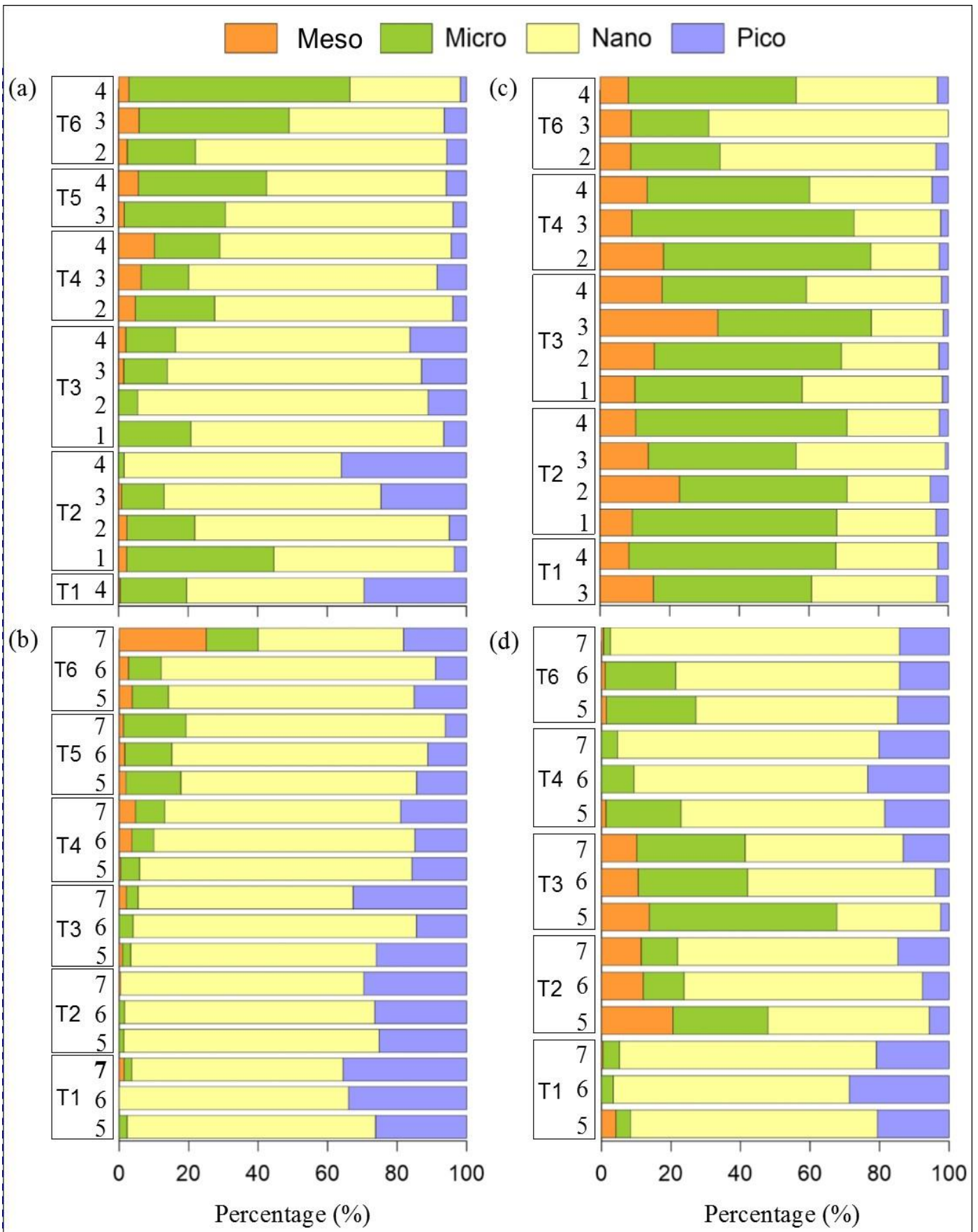
Supplementary Figure 2 - Vertical distribution of phosphate (mM) and silicate (mM) along various cross-shore transects in the EAS during the SWM.



Supplementary Figure 3 - A typical flow cytogram of pico- and nano-phytoplankton



Supplementary Figure 4 - FlowCAM images of micro-phytoplankton during (a) NEM and (b) SWM



Supplementary Figure 5 - Percentage contribution of phytoplankton size classes during the NEM (a) coastal, (b) offshore and the SWM (c) coastal, (d) offshore.

(a)

	SST	NO ₃	PO ₄	SiO ₄	N:P	Si:N	MACRO	MICRO	NANO	PICO
SST	1									
NO ₃	-0.46	1								
PO ₄	-0.74	0.83	1							
SiO ₄	-0.51	0.8	0.78	1						
N:P	-0.26	0.77	0.51	0.56	1					
Si:N	0.35	-0.2	-0.29	-0.06	-0.51	1				
MESO	-0.59	0.34	0.41	0.36	0.24	-0.2	1			
MICRO	-0.66	0.48	0.44	0.37	0.01	-0.04	0.39	1		
NANO	-0.62	0.43	0.52	0.59	0.23	-0.22	0.42	0.53	1	
PICO	0.16	-0.25	-0.37	-0.34	-0.04	-0.35	0.08	-0.16	0.14	1

(b)

	SST	NO ₃	PO ₄	SiO ₄	N:P	Si:N	MESO	MICRO	NANO	PICO
SST (°C)	1									
NO ₃	-0.74	1								
PO ₄	-0.76	0.96	1							
SiO ₄	-0.75	0.67	0.64	1						
N:P	-0.63	0.85	0.77	0.71	1					
Si:N	-0.47	0.15	0.16788	0.74	0.16	1				
MESO	-0.38	0.36	0.37	0.35	0.26	0.37	1			
MICRO	-0.36	0.35	0.38	0.18	0.24	0.26	0.8	1		
NANO	0.21	0.17	0.2	0.09	0.18	0.22	0.83	0.89	1	
PICO	0.23	-0.37	-0.36	-0.29	-0.15	-0.08	0.24	0.28	0.44	1

Supplementary Table 1 - Multiple correlations of physicochemical and biological parameters during (a) NEM and (b) the SWM